J. Math. Anal. Appl. 409 (2014) 119–139

Contents lists available at ScienceDirect

Journal of Mathematical Analysis and Applications

journal homepage: www.elsevier.com/locate/jmaa

Absolute flux optimising curves of flows on a surface

Sanjeeva Balasuriya [a,b,*], Gary Froyland [c], Naratip Santitissadeekorn [d]

[a] School of Mathematical Sciences, University of Adelaide, Adelaide SA 5005, Australia
[b] Department of Mathematics, Connecticut College, New London CT 06320, USA
[c] School of Mathematics and Statistics, University of New South Wales, Sydney NSW 2052, Australia
[d] Department of Mathematics, University of North Carolina, Chapel Hill NC 27599, USA

ARTICLE INFO

Article history:
Received 24 July 2012
Available online 29 June 2013
Submitted by Pengfei Yao

Keywords:
Minimum flux curves
Absolute flux
Weighted flux

ABSTRACT

Given a flow on a surface, we consider the problem of connecting two distinct trajectories by a curve of extremal (absolute) instantaneous flux. We develop a complete classification of flux optimal curves, accounting for the possibility of the flux having spatially and temporally varying weight. This weight enables modelling the flux of non-equilibrium distributions of tracer particles, pollution concentrations, or active scalar fields such as vorticity. Our results are applicable to all smooth autonomous flows, area preserving or not.

1. Introduction

Given a two-dimensional manifold Ω, possibly with nonempty boundary, and a C^2 function $\mathbf{f} : \Omega \to \mathbb{R}^2$ we consider the dynamical system

$$\dot{\mathbf{x}} = \mathbf{f}(\mathbf{x}) \tag{1}$$

in which $\mathbf{x} \in \Omega$. We will search for flux extremising curves that join a specified pair of points $\mathbf{a}$ and $\mathbf{b}$. The "flux" here will be a general quantity; our definitions will provide for the quantification of each of a variety of entities crossing the curve per unit time, including the quantity of fluid, heat or chemical, or the amount of vorticity or potential vorticity. Clearly if $\mathbf{a}$ and $\mathbf{b}$ lie on a single trajectory of the flow, one may travel along this trajectory from $\mathbf{a}$ to $\mathbf{b}$ and incur zero flux; this trajectory segment would be the flux minimising curve. To pose nontrivial questions about flux extremising curves, we need to restrict our attention to pairs of points than cannot be joined by trajectories. This leads us to the notion of an *integral set*. Let $\phi(\mathbf{x}, t)$ be the flow which is generated by (1); that is, $\phi(\mathbf{x}, t)$ is the location in Ω to which an initial condition $\mathbf{x}$ progresses by time t.

Definition 1 (*Closed Trajectory*)**.** For any $\mathbf{x} \in \Omega$, define its *closed trajectory* $T_{\mathbf{x}}$ by

$$T_{\mathbf{x}} := \overline{\{\phi(\mathbf{x}, t) : t \in \mathbb{R}\}}. \tag{2}$$

Definition 2 (*Integral Set*)**.** Define the sets $I^i_{\mathbf{x}}$ for $i \in \mathbb{N}$ inductively by

$$I^1_{\mathbf{x}} = T_{\mathbf{x}},$$
$$I^i_{\mathbf{x}} = \left\{\mathbf{y} \in \Omega : T_{\mathbf{y}} \cap I^{i-1}_{\mathbf{x}} \neq \emptyset\right\} \quad (i = 2, 3, 4, \ldots),$$

* Corresponding author at: School of Mathematical Sciences, University of Adelaide, Adelaide SA 5005, Australia.
E-mail address: sanjeevabalasuriya@yahoo.com (S. Balasuriya).

0022-247X/$ – see front matter
http://dx.doi.org/10.1016/j.jmaa.2013.06.013

and then the *integral set* $I_{\mathbf{x}}$ of $\mathbf{x}$ by

$$I_{\mathbf{x}} = \bigcup_{i\in\mathbb{N}} I^i_{\mathbf{x}}. \tag{3}$$

Thus, $I_{\mathbf{x}}$ includes all trajectories that can be connected to $\mathbf{x}$ by going through a countable number of "end states", such as fixed points or periodic orbits; connecting through an end state at infinity is not allowed. The set $I_{\mathbf{x}}$ may be either one- or two-dimensional, depending on the topology of Ω and the dynamics of (1). We will be concerned with pairs of points $\mathbf{a}$ and $\mathbf{b}$ with the property that any curve joining $\mathbf{a}$ to $\mathbf{b}$ must have nonzero absolute flux across it. Thus the integral sets through $\mathbf{a}$ and $\mathbf{b}$ should neither intersect, nor be connectable via a curve of fixed points:

Hypothesis 1.

(i) The integral sets $I_{\mathbf{a}}$ and $I_{\mathbf{b}}$ do not intersect, that is $I_{\mathbf{a}} \cap I_{\mathbf{b}} = \emptyset$, and
(ii) There does not exist a curve $\tilde{\mathcal{C}} \subseteq \Omega$ such that $\mathbf{f}(\mathbf{x}) = \mathbf{0}$ for all $\mathbf{x} \in \tilde{\mathcal{C}}$, and for which $I_{\mathbf{a}} \cap \tilde{\mathcal{C}}$ and $I_{\mathbf{b}} \cap \tilde{\mathcal{C}}$ are both nonempty.

We will define flux in relation to a non-negative time-varying weight function g. The basic example to keep in mind is that $g(\mathbf{x}, t)$ is a chemical concentration; the flux definitions will then compute the flux of the chemical (in chemical mass per unit time, say), at each instance in time. Note that we allow g to vary with time; this enables the flux computations even when the chemical concentration is not in equilibrium. As will be argued later, our definition for g will allow the modelling of more general situations, such as the flux of vorticity or temperature. Our weight function is in general defined by:

Definition 3 (*Weight Function*)**.** The *weight function* $g : \Omega \times \mathbb{R} \to [0, \infty)$ is such that $g(\cdot, t) \in C^1(\Omega)$ for any $t \in \mathbb{R}$.

At a fixed time t, the idea is to determine curves which extremise the flux; these curves are restricted to C^1 curves in Ω taking the form $\mathcal{C} = \{\mathbf{r}(p) : 0 \le p \le 1\}$. The following definitions for the flux are at a specific time instance t, and are therefore *instantaneous* in nature.

Definition 4 (*Weighted Local (Point) Flux*)**.** The *weighted local flux* (or *weighted point flux*) at differentiable points $\mathbf{r}(p)$ on a piecewise C^1 curve $\mathcal{C} = \{\mathbf{r}(p) : 0 \le p \le 1\} \subset \Omega$ at a time instance t is given by

$$L_g(\mathbf{r}(p), t) := g(\mathbf{r}(p), t)\, \mathbf{f}(\mathbf{r}(p)) \cdot J\mathbf{r}'(p), \tag{4}$$

where $J := \begin{pmatrix} 0 & -1 \\ 1 & 0 \end{pmatrix}$.

Since $J\mathbf{r}'(p)$ represents the leftwards-pointing normal direction when traversing the curve in the direction of increasing p, the local flux measures the strength of $g\mathbf{f}$ in the leftwards normal direction to the curve, weighted according to g. Integrating the local flux over a curve $\mathcal{C}$ gives the "weighted flux" across $\mathcal{C}$, in the following senses:

Definition 5 (*Weighted Signed Flux*)**.** The *weighted signed flux* $F^s_g(\mathcal{C}, t)$ across $\mathcal{C}$ at a time instance t is defined by

$$F^s_g(\mathcal{C}, t) := \int_0^1 \mathbf{f}(\mathbf{r}(p)) \cdot J\frac{\mathbf{r}'(p)}{|\mathbf{r}'(p)|} \left|\mathbf{r}'(p)\right| g(\mathbf{r}(p), t)\, \mathrm{d}p = \int_0^1 L_g(\mathbf{r}(p), t)\, \mathrm{d}p. \tag{5}$$

Definition 6 (*Weighted Absolute Flux*)**.** The *weighted absolute flux* $F^a_g(\mathcal{C}, t)$ across $\mathcal{C}$ at a time instance t is defined by

$$F^a_g(\mathcal{C}, t) := \int_0^1 \left|\mathbf{f}(\mathbf{r}(p)) \cdot J\frac{\mathbf{r}'(p)}{|\mathbf{r}'(p)|}\right| \left|\mathbf{r}'(p)\right| g(\mathbf{r}(p), t)\, \mathrm{d}p = \int_0^1 \left|L_g(\mathbf{r}(p), t)\right| \mathrm{d}p. \tag{6}$$

The "standard flux" (quantity of fluid crossing per unit time) is obtained by setting $g \equiv 1$, while more general g can be used to represent the flux associated with a passively transported chemical concentration or of a (passive or active) scalar field. To state our main result, we also need the following definitions.

Definition 7 (*Weighted Compressibility*)**.** The *weighted compressibility* function $\kappa_g : \Omega \times \mathbb{R} \to \mathbb{R}$ is defined by

$$\kappa_g(\mathbf{x}, t) := \nabla \cdot (\mathbf{f}(\mathbf{x}) g(\mathbf{x}, t)), \tag{7}$$

where ∇ denotes the derivative with respect to $\mathbf{x}$.

If $g \equiv 1$, the weighted compressibility becomes the divergence of the vector field (the compressibility of the flow). That is, $\kappa_1 = \nabla \cdot \mathbf{f}$.

Definition 8 (*Flow Derivative*)**.** The *flow derivative* of a scalar field $h(\mathbf{x}, t)$ on $\Omega \times \mathbb{R}$ which is C^1 in Ω for each $t \in \mathbb{R}$ is given by

$$D_{\mathbf{f}} h(\mathbf{x}, t) := \mathbf{f}(\mathbf{x}) \cdot \nabla h(\mathbf{x}, t). \tag{8}$$

The flow derivative is equivalent to the *material derivative* (derivative following the flow of (1)) for time-independent functions. Leaving the formalities of "local" for later, our main result is

Theorem 1. *A piecewise C^1 simple curve $\mathcal{C}$ connecting $I_{\mathbf{a}}$ to $I_{\mathbf{b}}$ at an instantaneous time t is:*

1. *locally weighted absolute flux minimal iff*
   (a) *$\mathcal{C}$ is on the "entry boundary"*[1] *of Ω and satisfies $\mathcal{C} \subseteq \{\mathbf{x} \in \Omega : \kappa_g(\mathbf{x}, t) > 0\}$,*
   (b) *$\mathcal{C}$ is on the "exit boundary" of Ω and satisfies $\mathcal{C} \subseteq \{\mathbf{x} \in \Omega : \kappa_g(\mathbf{x}, t) < 0\}$.*
   (c) *$\mathcal{C}$ in the interior of Ω and satisfies $\mathcal{C} \subseteq \{\mathbf{x} \in \Omega : \kappa_g(\mathbf{x}, t) = 0, D_{\mathbf{f}}\kappa_g(\mathbf{x}, t) > 0\}$,*
2. *locally weighted absolute flux maximal iff*
   (a) *$\mathcal{C}$ is on the "entry boundary" of Ω and satisfies $\mathcal{C} \subseteq \{\mathbf{x} \in \Omega : \kappa_g(\mathbf{x}, t) < 0\}$,*
   (b) *$\mathcal{C}$ is on the "exit boundary" of Ω and satisfies $\mathcal{C} \subseteq \{\mathbf{x} \in \Omega : \kappa_g(\mathbf{x}, t) > 0\}$.*
   (c) *$\mathcal{C}$ in the interior of Ω and satisfies $\mathcal{C} \subseteq \{\mathbf{x} \in \Omega : \kappa_g(\mathbf{x}, t) = 0, D_{\mathbf{f}}\kappa_g(\mathbf{x}, t) < 0\}$.*

If $\kappa_g \equiv 0$ on Ω we are in a degenerate situation where all curves joining $I_{\mathbf{a}}$ to $I_{\mathbf{b}}$ have equal weighted signed flux.

Related work includes that of MacKay [27], who considers signed and absolute flux (with $g \equiv 1$) for volume-preserving three-dimensional flows. MacKay concludes that a surface S has locally stationary signed flux iff ∂S is invariant under the flow, and that a surface S has locally minimal absolute flux iff S can be decomposed into surfaces through which the flow is unidirectional and if there are no rapid changes of flow direction ("sneaky returns"). The questions we pose in this present work are related, but rather different. Firstly, MacKay's setting [27] is "degenerate" in our framework and all connecting curves incur the same flux. We generalise this degenerate setting from area-preserving flows to flows preserving any invariant density, and show that this degeneracy persists when the weight function g is chosen to equal the invariant density, representing the long-term asymptotic distribution of points on trajectories. In the area-preserving case, we set $g \equiv 1$ to obtain this degeneracy. Secondly, we consider the interesting case where the flux weight is not matched to the invariant density. Such a situation arises for example, when considering "standard" flux for a non-area-preserving flow, or when considering the transport of tracer particles in fluid where the distribution of the tracers is not uniform, nor in equilibrium. Thirdly, as many models arising in applications from geophysical or mechanical fluid flow involve domains with boundaries, we include an analysis of the variation of flux at or near boundaries.

Minimum flux curves from the perspective of standard maps on a cylinder have been addressed by Polterovich [35]. The idea was to determine a closed nonintersecting curve homotopic to a cycle across which the transport of Lebesgue measure under one iteration of the map was minimal; equivalently, the partitioning of the cylinder into two regions such that the interchange of Lebesgue mass by the map is minimal. Polterovich demonstrated the construction of such a flux minimising curve for sufficiently large parameter values of the standard map, by connecting together smooth arcs related to stable and unstable manifolds [35]. Thus, in this particular situation flux-minimising curves can be highly complex. Our situation is quite different in that we examine a flow as opposed to a map, we do not confine our analysis to cylinders, our prospective curves connect together two specific points as opposed to being closed curves, and we define our flux in terms of the flow across the curve of interest. As stated in Theorem 1, our flux-minimising curves are much smoother entities, which in unsurprising since we consider a flow.

The determination of minimal transport barriers has also been considered from the ergodic-theoretic or probabilistic point of view, where the basic mathematical tool is the Perron–Frobenius operator (or its generator) for the flow. In this setting, one typically seeks "almost-invariant" sets [14,17–19]; namely sets with a low probability of trajectories leaving the set. These almost-invariant sets mitigate transport throughout the full phase space and provide a skeleton around which faster mixing dynamics occurs. Almost-invariant set analysis has been applied to ocean flows [13,21], where almost-invariant sets delimit stable structures such as gyres and eddies; to periodically forced flows [38] where almost-invariant (almost-cyclic) sets describe coherent periodic regions ("ghost rods") connected with stirring; to astrodynamics [15], where almost-invariant sets are regions from which asteroid escape is rare; and to molecular dynamics [16,36], where almost-invariant sets are stable molecular configurations. Related approaches include [9,30], where function values along long trajectories are used to decompose the phase space into invariant regions. When the underlying dynamics is a flow, the only possibility for the departure of trajectories from a set is through the boundary of the set. Co-dimension 1 invariant manifolds provide impenetrable barriers for trajectories and intuitively may seem likely to form (partial) boundaries of almost-invariant sets. Invariant manifolds cannot provide *full* boundaries in transitive flows, (e.g., the steady three-dimensional Lorenz equations with standard parameters [26]), as transitivity precludes the existence open invariant sets. Nevertheless, numerical work [20] suggests that the boundaries of almost-invariant sets contain significant portions of "fundamental" invariant manifolds: those associated with fixed points or the lowest period orbits. Thus, our new analytic determination of curves with minimal absolute flux has the potential to help find a theoretical link between geometric transport barriers (co-dimension 1 curves in phase space) and almost-invariant sets.

Extremising flux is important in nano/micro-fluidics, where efficient mixing is desirable for improved performance of micro-fluidic devices which operate in the low Reynolds number regime. In addition to multitudinous numerical and experimental quantifications of flux, there are a few theoretical tools to help maximise mixing measures [10,11,22,25,29,39],

[1] The entry boundary of Ω is the part of $\partial\Omega$ with the vector field $\mathbf{f}$ pointing towards the interior of Ω (we assume that the vector field $\mathbf{f}$ can be smoothly extended to a small open neighbourhood of Ω); the exit boundary of Ω is the part of $\partial\Omega$ with the vector field $\mathbf{f}$ pointing out of Ω.

or the flux across given flow separators [5–8]. This article addresses a complementary theoretical issue: determining the "flow separator" across which flux is extremal, as is also the focus in [27,28].

As demonstrated in [40], a flux extremising geometric flow method is also relevant in blood vessel segmentation in 2D and 3D in angiography data. A solution of such problem is down to finding a way to optimally move a closed curve so that the inward normals to the curve are everywhere aligned with the direction of a given (steady) vector field as much as possible, hence maximising the total inward flux.

Studying two-dimensional flows on manifolds as is done in this article also has applicability for three-dimensional flows in several situations. Firstly, consider steady Euler flows, for which Arnold [2,3] established integrability, with motion restricted on two-dimensional manifolds associated with level sets ("Lamb surfaces") of the Bernoulli function [23,37]. Secondly, the barotropic assumption in oceanography [33] confines motion to isopycnal (constant density) surfaces; to a good approximation, flow in the open ocean is on slightly deformed parallel sheets. In both these examples, incompressibility of the fully three-dimensional flow does not automatically imply area-preservation (i.e., $\kappa_1 = 0$) in the two-dimensional invariant surfaces, making the framework of the current article additionally relevant. The tiny cross-stream dimensions of many micro-fluidic devices provides a third example of a situation in which two-dimensional flow is a good approximation, in which moreover the concept of maximising fluid mixing is crucially important in improving reaction rates (cf. [12,31]).

An outline of the paper is as follows. In Section 2 we consider the variation of instantaneous flux when perturbing a curve either in, or against, the direction of the flow. Section 3 builds on the results developed in Section 2 to construct necessary and sufficient conditions for curves to be locally flux minimal or maximum under perturbation. Section 4 considers the special case in which the weighted compressibility is zero, which includes, for example, incompressible flows. Section 5 discusses the role of the weight function g, including the degenerate situation where g is a multiple of the invariant density of the flow, or when it corresponds to a non-equilibrium tracer concentration or vorticity field. Proofs are given in the Appendix.

2. Absolute flux and perturbed curves

We begin by demonstrating some basic responses of flux over a curve $\mathcal{C}$ when the curve is perturbed in ways that are naturally related to the underlying flow.

Definition 9 (*Uni-Directional*)**.** Let $\mathcal{C}$ be a piecewise differentiable curve of non-zero length, parametrisable by $\mathbf{r}(p)$ where $p \in [0, 1]$. Let L_1 be the point flux associated with $g = 1$. Then at time t we say,

- the flow across $\mathcal{C}$ is *uni-directional* if for all p_1 and p_2 in $[0, 1]$ at which $\mathbf{r}(p)$ is differentiable,

$$L_1(\mathbf{r}(p_1), t)\, L_1(\mathbf{r}(p_2), t) > 0.$$

- the flow across $\mathcal{C}$ is *essentially uni-directional* if for all p_1 and p_2 in $[0, 1]$ at which $\mathbf{r}(p)$ is differentiable,

$$L_1(\mathbf{r}(p_1), t)\, L_1(\mathbf{r}(p_2), t) \geq 0.$$

While uni-directionality ensures that the flow across the curve is "in the same direction" at each point on the curve, essential uni-directionality permits the piecewise differentiable function $L_1(\mathbf{r}(p), t)$ to be zero at points or on intervals in p, corresponding to situations in which the curve is tangential to the vector field $\mathbf{f}$.

Definition 10 (*Weighted Compressibility Partition*)**.** Define

$$\begin{aligned} K_g(t) &:= \left\{\mathbf{x} \in \Omega : \kappa_g(\mathbf{x}, t) = 0\right\} \\ K_g^p(t) &:= \left\{\mathbf{x} \in \Omega : \kappa_g(\mathbf{x}, t) > 0\right\} \\ K_g^n(t) &:= \left\{\mathbf{x} \in \Omega : \kappa_g(\mathbf{x}, t) < 0\right\} \end{aligned} \tag{9}$$

Clearly, $K_g^p \cup K_g^n \cup K_g = \Omega$, and we begin by considering the flux response of perturbations of curves lying within either $K_g^p(t)$ or $K_g^n(t)$. The following definition is needed to define the class of permitted perturbations.

Definition 11 ($\mathcal{C}$*-Generated Curves*)**.** Let $\mathcal{C}$ be a simple piecewise differentiable finite curve segment, across which the flow is unidirectional at a time instance t. Let $\mathcal{C}$ be parametrised by $\mathbf{r}(p)$ where $0 \leq p \leq 1$. Then, the class of $\mathcal{C}$*-generated curves* are those curves $\mathcal{C}_\tau$ given by

$$\mathcal{C}_\tau := \{\mathbf{y} \in \Omega : \mathbf{y} = \phi(\mathbf{x}, \tau(\mathbf{x})) \text{ for } \mathbf{x} \in \mathcal{C}\}, \tag{10}$$

for continuous and piecewise differentiable functions $\tau : \mathcal{C} \to \mathbb{R}$.

A $\mathcal{C}$-generated curve is thus formed by following the flow of each point on $\mathcal{C}$ along its trajectory fibre for some specified time (which can be different for each point), to obtain a collection of points. Given a curve $\mathcal{C} \in \Omega$ we define neighbourhoods (called fattening sets) of $\mathcal{C}$ by flowing forward and backward in time.

Definition 12 (*Positive and Negative Fattening Sets*)**.** Let $\mathcal{C}$ be a simple piecewise differentiable finite curve segment with its two endpoints being on $I_{\mathbf{a}}$ and $I_{\mathbf{b}}$ respectively, and suppose the flow is unidirectional across $\mathcal{C}$ at time t. Let $T_+ > 0$ and $T_- < 0$ be piecewise C^1 functions defined on $\mathcal{C}$.

- A *positive fattening set* S_{T_+} of $\mathcal{C}$ is defined to be the region bounded by the curves $I_{\mathbf{a}}$, $I_{\mathbf{b}}$, $\mathcal{C}$ and the $\mathcal{C}$-generated curve $\mathcal{C}_{T_+} = \{\mathbf{y} = \phi(\mathbf{x}, T_+(\mathbf{x})) \in \Omega \text{ for } \mathbf{x} \in \mathcal{C}\}$, in which S_{T_+} includes the boundaries along $I_{\mathbf{a}}$, $I_{\mathbf{b}}$, but not along $\mathcal{C}$ and $\mathcal{C}_{T_+}$.
- A *negative fattening set* S_{T_-} of $\mathcal{C}$ is defined to be the region bounded by the curves $I_{\mathbf{a}}$, $I_{\mathbf{b}}$, $\mathcal{C}$ and the $\mathcal{C}$-generated curve $\mathcal{C}_{T_-} = \{\mathbf{y} = \phi(\mathbf{x}, T_-(\mathbf{x})) \in \Omega \text{ for } \mathbf{x} \in \mathcal{C}\}$, in which S_{T_-} includes the boundaries along $I_{\mathbf{a}}$, $I_{\mathbf{b}}$, but not along $\mathcal{C}$ and $\mathcal{C}_{T_-}$.

We will call a positive or negative fattening set *permissible* if it is a subset of Ω.

Lemma 1 (*One-Sided Flux Optimisation*)**.** *Let $\mathcal{C}$ be a piecewise C^1 curve segment across which the flow is uni-directional at time t.*

1. *Let $\mathcal{C} \in K_g^p(t)$.*
   - *All $\mathcal{C}$-generated curves $\mathcal{C}_\tau$ in a permissible positive fattening set in $K_g^p(t)$ have greater absolute flux; that is, $F_g^a(\mathcal{C}, t) < F_g^a(\mathcal{C}_\tau, t)$. Thus $\mathcal{C}$ is a one-sided flux minimising curve in relation to forward-time deformations of $\mathcal{C}$.*
   - *All $\mathcal{C}$-generated curves $\mathcal{C}_\tau$ in a permissible negative fattening set in $K_g^p(t)$ have lower absolute flux; that is, $F_g^a(\mathcal{C}, t) > F_g^a(\mathcal{C}_\tau, t)$. Thus $\mathcal{C}$ is a one-sided flux maximising curve in relation to backward-time deformations of $\mathcal{C}$.*
2. *Let $\mathcal{C} \in K_g^n(t)$.*
   - *All $\mathcal{C}$-generated curves $\mathcal{C}_\tau$ in a permissible negative fattening set in $K_g^n(t)$ have greater absolute flux; that is, $F_g^a(\mathcal{C}, t) < F_g^a(\mathcal{C}_\tau, t)$. Thus $\mathcal{C}$ is a one-sided flux minimising curve in relation to backward-time deformations of $\mathcal{C}$.*
   - *All $\mathcal{C}$-generated curves $\mathcal{C}_\tau$ in a permissible positive fattening set in $K_g^n(t)$ have lower absolute flux; that is, $F_g^a(\mathcal{C}, t) > F_g^a(\mathcal{C}_\tau, t)$. Thus $\mathcal{C}$ is a one-sided flux maximising curve in relation to forward-time deformations of $\mathcal{C}$.*

Proof. See Appendix A.2. □

The point of Lemma 1 is that it provides sufficient conditions for a curve $\mathcal{C}$ (in e.g. the first dot point of the lemma) to "get worse" (have greater flux) when perturbed (generated) by flowing *forward* in time. For example, if Ω has a *boundary* over which flow is "entering" Ω (we assume that the vector field can be smoothly extended to a small open neighbourhood of Ω and on $\partial\Omega$ the vector field points towards the interior of Ω) and a segment $\mathcal{C}$ of this boundary joins $I_{\mathbf{a}}$, $I_{\mathbf{b}}$ and satisfies $\mathcal{C} \in K_g^p(t)$, then $\mathcal{C}$ (i.e., part of the boundary of Ω) has the potential to be a *global* flux minimising curve joining $I_{\mathbf{a}}$, $I_{\mathbf{b}}$. Similar considerations hold for boundaries of Ω where the flow "exits" Ω.

We demonstrate the application of Lemma 1 via two straightforward examples in which g is time-independent, postponing a time-dependent example to the next section.

Example 1 (*Horizontal Flow on a Square*)**.** Let $\Omega = [0, 1] \times [0, 1]$ and set $\mathbf{f}(x, y) = ((x + y - 1)^2 + \delta, 0)$, $\delta > 0$. Suppose $\mathbf{a} = (a_x, 0)$ and $\mathbf{b} = (b_x, 1)$ for some $a_x, b_x \in [0, 1]$. Then $I_{\mathbf{a}} = [0, 1] \times \{0\}$ and $I_{\mathbf{b}} = [0, 1] \times \{1\}$ satisfy Hypothesis 1. Let g be associated with a uniform equilibrium concentration of a chemical which is passively advected by the flow; set $g = \beta$ (a positive constant). We have $K_g^p = \{y > -x + 1\} \cap \Omega$ and $K_g^n = \{y < -x + 1\} \cap \Omega$ for all t. Lemma 1 shows that the "entry" boundary $\mathcal{C}_{entry} = \{0\} \times [0, 1]$ is a one-sided (forward time, to the right) flux maximiser and the "exit" boundary $\mathcal{C}_{exit} = \{1\} \times [0, 1]$ is a one-sided (backward time, to the left) flux maximiser. The flux (mass of chemical crossing per unit time) across both $\mathcal{C}_{entry}$ and $\mathcal{C}_{exit}$ is $\beta\,(1/3 + \delta)$. □

Example 2 (*Duffing*)**.** Consider the modified Duffing equation

$$\ddot{x} - x + x^3 - \epsilon x y = 0,$$

with $\epsilon > 0$, which can be written as a system as

$$\left.\begin{aligned} \dot{x} &= y \\ \dot{y} &= x - x^3 + \epsilon x y \end{aligned}\right\}. \tag{11}$$

We consider $\Omega = \{(x, y) : x, y \geq 0\}$, and let $g = 1$. There are two fixed points in Ω: a saddle at $\mathbf{a} = (0, 0)$ and a source at $(1, 0)$. For small ϵ, $I_{\mathbf{a}}$ is the segment of unstable manifold beginning at $\mathbf{a}$ and ending at a point on the x-axis beyond $\sqrt{2}$, say at $\mathbf{d} = (0, d)$. We choose $\mathbf{b} = (\sqrt{2}, 0)$[2]; $I_{\mathbf{b}}$ is the backward trajectory from $(\sqrt{2}, 0)$ to some point $\mathbf{c} = (c, 0)$, $c > 0$. The sets $I_{\mathbf{a}}$, $I_{\mathbf{b}}$ satisfy Hypothesis 1, see Fig. 1. By Lemma 1, since K_g^p is the open right hand plane, the line segment $\mathbf{a}$ to $\mathbf{c}$ (the "entry" boundary) is a one-sided flux minimising curve. Similarly, the line joining $\mathbf{b}$ to $\mathbf{d}$ (the "exit" boundary) is a one-sided flux maximising curve. For $\epsilon = 0.1$, the fluxes across these two boundaries are respectively $c^2(c^2 - 2)/4 \approx 0.04983$, where $c \approx 0.32433$, and $(d^2(d^2 - 2) - b^2(b^2 - 2))/4 \approx 0.06223$, where $b = \sqrt{2}$ and $d \approx 1.45518$. □

We have not yet discussed the situation where $\mathcal{C} \in K_g(t)$, but the intuition from Lemma 1 is that under suitable additional conditions, such $\mathcal{C}$ would be candidates for two-sided local absolute flux minimising or maximising curves. In the next section we develop these additional conditions.

[2] If $\epsilon = 0$ the unstable manifold of $\mathbf{a}$ passes through $\mathbf{b}$.

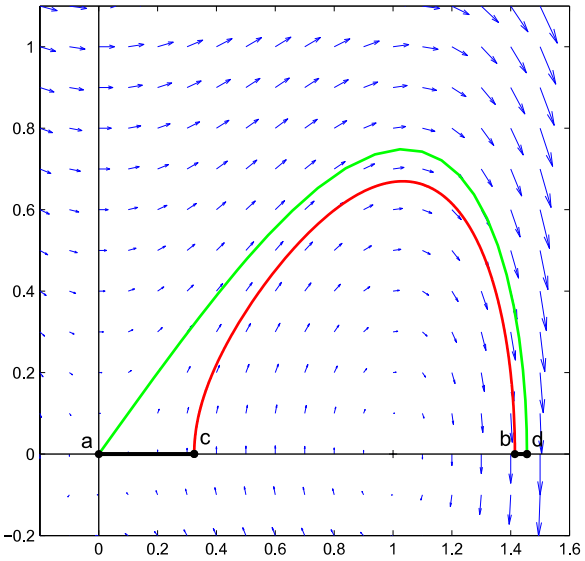

Fig. 1. The sets $I_{\mathbf{a}}$ (in green) and $I_{\mathbf{b}}$ (in red), and the entry and exit boundaries (in black) in Example 2 with $\epsilon = 0.1$. (For interpretation of the references to colour in this figure legend, the reader is referred to the web version of this article.)

3. Local absolute flux optimising curves

In this section, we examine curves which *locally* minimise and maximise the absolute flux.

3.1. Local absolute flux minimising curves

We will show that absolute flux minimising curves are associated with the zero weighted compressibility set $K_g(t)$. Generically, at each instance in time $K_g(t)$ is either a connected curve or a finite union of such connected curves. If the flow (1) is area-preserving (Hamiltonian) for all times and $g = 1$, then $K_g = \Omega$ which requires special consideration.

Definition 13 (*Weighted Compressibility-Increasing Subset*)**.** The *weighted compressibility-increasing* subset $K_g^+(t)$ of $K_g(t)$ is defined by

$$K_g^+(t) := \left\{\mathbf{x} \in K_g(t) : \mathbf{f} \cdot \nabla \kappa_g(\mathbf{x}, t) > 0\right\} := \left\{\mathbf{x} \in K_g : D_{\mathbf{f}} \kappa_g(\mathbf{x}, t) > 0\right\}. \tag{12}$$

Hypothesis 2. The sets $I_{\mathbf{a}}$, $I_{\mathbf{b}}$, $K_g(t)$ and $K_g^+(t)$ are such that

- $K_g(t)$ is one-dimensional,
- $K_g^+(t)$ is one-dimensional, and
- There exists a point in $I_{\mathbf{a}} \cap K_g^+(t)$ and a point in $I_{\mathbf{b}} \cap K_g^+(t)$ that can be connected by a piecewise C^1-smooth simple curve segment $\mathcal{C}_+ \subseteq K_g^+(t) \subseteq K_g(t)$ of positive length.
- $\mathcal{C}_+$ lies in the interior of Ω.

We restrict our attention to times t for which Hypothesis 2 is met, and note that the curve $\mathcal{C}_+$ depends on t (but this dependence will be suppressed for notational brevity). The picture associated with Hypothesis 2 is given in Fig. 2. Let $\mathbf{r}_+(p)$, $0 \le p \le 1$, be a parametrisation for $\mathcal{C}_+$ such that $\mathbf{r}_+(0)$ is the intersection point of $\mathcal{C}_+$ with $I_{\mathbf{a}}$, and $\mathbf{r}_+(1)$ is the intersection point with $I_{\mathbf{b}}$.

Lemma 2 (*Uni-Directional Flux*)**.** *The flow across $\mathcal{C}_+$ is uni-directional at time t.*

Proof. See Appendix A.3. □

Definition 14 (*Fattening Set*)**.** Let $T_+(\mathbf{x}) > 0$ and $T_-(\mathbf{x}) < 0$ be continuous and piecewise differentiable functions defined on $\mathcal{C}_+$, such that $\phi(\mathbf{x}, T_+(\mathbf{x})) \subseteq \Omega$ and $\phi(\mathbf{x}, T_-(\mathbf{x})) \subseteq \Omega$. We define the *fattening set* S_T of $\mathcal{C}_+$ to be the union of the associated positive and negative fattening sets, i.e., the region bounded by the curves $I_{\mathbf{a}}$ and $I_{\mathbf{b}}$, and the two $\mathcal{C}_+$-generated curves

$$\mathcal{C}_{T_+} = \{\phi(\mathbf{x}, T_+(\mathbf{x})) : \text{ for } \mathbf{x} \in \mathcal{C}_+\} \quad \text{and} \quad \mathcal{C}_{T_-} = \{\phi(\mathbf{x}, T_-(\mathbf{x})) : \text{ for } \mathbf{x} \in \mathcal{C}_+\}$$

in which S_T includes the boundaries along $I_{\mathbf{a}}$ and $I_{\mathbf{b}}$, but not the boundaries along $\mathcal{C}_{T_+}$ and $\mathcal{C}_{T_-}$. The fattening set is *permissible* if it is contained in Ω.

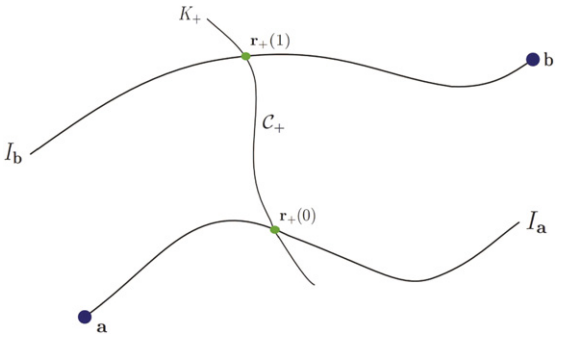

Fig. 2. Intersection pattern needed for flux-minimising result.

Given the strict positivity of T_+ and the strict negativity of T_-, the fattening set defines an expansion of $\mathcal{C}_+$ in the directions of the fibres associated with the trajectories passing through $\mathcal{C}_+$. Such a fattening set exists since $\mathcal{C}_+$ is in the interior of Ω, and thus permissible positive and negative fattening sets exist. Since Lemma 2 guarantees a non-zero uni-directional flow at all points on $\mathcal{C}_+$, a fattening set is the union over $\mathbf{x} \in \mathcal{C}_+$ of open curve segments lying along trajectories of (1) between $\phi(\mathbf{x}, T_-(\mathbf{x}))$ and $\phi(\mathbf{x}, T_+(\mathbf{x}))$.

Definition 15 (*Non-Degenerate Fattening*)**.** A fattening set S_T of $\mathcal{C}_+$ is called *non-degenerate* if it is permissible and

(a) The flow across any $\mathcal{C}_+$-generated curve $\mathcal{C}_\tau$ in S_T is essentially uni-directional, and
(b) $K_g(t) \cap S_T = \mathcal{C}_+$, i.e., there are no points in S_T except for those on $\mathcal{C}_+$ at which $\kappa_g = 0$.

Lemma 3 (*Existence of Non-Degenerate Fattening Set*)**.** *There exists a non-degenerate fattening set of $\mathcal{C}_+$, that is, there exist continuous functions $T_+(\mathbf{x}) > 0$ and $T_-(\mathbf{x}) < 0$ such that the corresponding fattening set S_T of $\mathcal{C}_+$ satisfies Definition 15.*

Proof. See Appendix A.4. □

Proposition 1 (*Flux-Minimising $\mathcal{C}_+$-Generated Curve*)**.** *Let S_T be a non-degenerate fattening set of $\mathcal{C}_+$, as guaranteed by Lemma 3. Then, for all $\mathcal{C}_+$-generated curves $\mathcal{C}_\tau \neq \mathcal{C}_+$ in S_T, $\mathcal{C}_+$ has the smallest absolute flux at time t, i.e.,*

$$F_g^a(\mathcal{C}_+, t) < F_g^a(\mathcal{C}_\tau, t).$$

Proof. See Appendix A.5. □

Theorem 2 (*Flux-Minimising Curve*)**.** *Let S_T be a non-degenerate fattening set of $\mathcal{C}_+$, as guaranteed by Lemma 3. Of all piecewise differentiable continuous curves which connect a point on $I_\mathbf{a}$ to a point on $I_\mathbf{b}$ while remaining in S_T, $\mathcal{C}_+$ has the smallest absolute flux at time t, i.e.,*

$$0 < F_g^a(\mathcal{C}_+, t) < F_g^a(\mathcal{C}, t)$$

for any piecewise differentiable curve $\mathcal{C} \neq \mathcal{C}_+$ in S_T which connects $I_\mathbf{a}$ to $I_\mathbf{b}$.

Proof. See Appendix A.6. □

The time-dependence t appearing in Theorem 2 is in the form of a parameter representing the weight function's t-dependence. The evolution of flux-minimising curves can be determined by identifying how $\mathcal{C}_+$ changes with t. This is examined in detail for certain classes of weight functions which are advected by the flow in Section 5.

Example 3 (*Horizontal Flow on a Square (Cont.)*)**.** We continue Example 1. One has $K_g = K_g^+ = \{y = -x + 1 : 0 \le x, y \le 1\}$, satisfying Hypothesis 2. By Theorem 2, $\mathcal{C} = K_g$ is a local flux minimising curve with total flux of $\beta\delta$. Combining this result with those of Example 1 we see that the local[3] flux maximising curves occur at each vertical boundary of the square domain Ω (with flux $\beta(1/3 + \delta)$) and the global flux minimising curve equal K_g (with flux $\beta\delta$). □

Example 4. Let $\mathbf{f}(x, y) = (-x - 2y + x^2, 2x - y - y^2)$ and set $g = 1$ to quantify the fluid amount transferred per unit time. The global features of the flow under this vector field are a (counterclockwise) spiral sink and a saddle; see Fig. 3.

It is straightforward to verify that K_g is the line $y = x - 1$. One has $\mathbf{f} \cdot \nabla\kappa_g = (-x - 2y + x^2, 2x - y - y^2) \cdot (2, -2) = -6x - 2y + 2x^2 + 2y^2$. Thus, the zero-level-set of $D_\mathbf{f}\kappa_g = \mathbf{f} \cdot \nabla\kappa_g$ is a circle centred at $(3/2, 1/2)$ with radius $\sqrt{10}/2$. The

[3] These are in fact *global* flux maximising curves in view of Section 3.2.

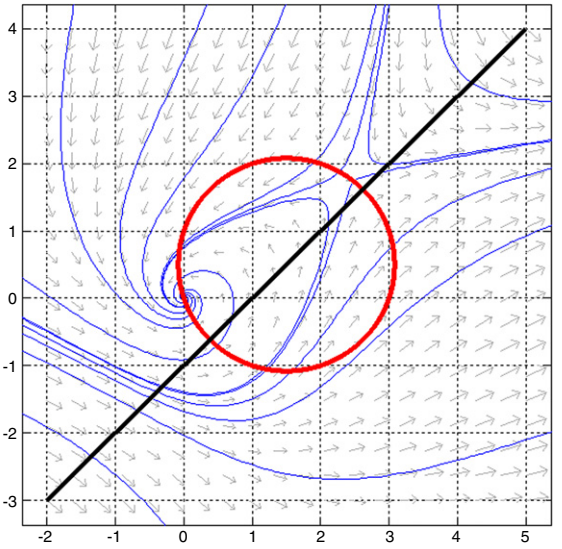

Fig. 3. Trajectories of the flow generated by the vector field $\mathbf{f}(x, y) = (-x - 2y + x^2, 2x - y - y^2)$ in blue. The straight black line is the zero divergence set K_g. The set K_g^p is the region below the black line and the set K_g^n is the region above the black line. The red circle is the zero-level-set of $\mathbf{f} \cdot \nabla\kappa_g$. The interior of the disc bounded by the black circle has $\mathbf{f} \cdot \nabla\kappa_g < 0$ and the complement of the closed disc has $\mathbf{f} \cdot \nabla\kappa_g > 0$. Thus K_g^+ is the portion of the black line outside the red circle and K_g^- is the portion of the black line inside the red circle. (For interpretation of the references to colour in this figure legend, the reader is referred to the web version of this article.)

interior of this circle has $D_{\mathbf{f}}\kappa_g < 0$ and $D_{\mathbf{f}}\kappa_g > 0$ on the complement of this closed disc. Thus K_g^+ is the line $y = x - 1$ intersected with the complement of the closed disc $(x - 3/2)^2 + (y - 1/2)^2 \leq 5/2$, a nonempty set. By Theorem 2 all piecewise differentiable local flux minimising curves have to be subsets of these two line segments. Suppose we excise a small open neighbourhood of the origin from Ω. Now, if **a**, **b** do not lie on the same trajectory, then $I_{\mathbf{a}} \neq I_{\mathbf{b}}$. Suppose the trajectories of **a** and **b** pass through the lower left part of Fig. 3 and cross the black line in the same direction (left to right), *outside* the black circle. If we wish to connect **a** and **b** in a flux minimal way, then by Theorem 2 we should follow the trajectory of **a** until the black line, then move along the black line to the trajectory of **b** and then follow this trajectory to the point **b**. If these trajectories cross the black line in the same direction (below to above) *inside* the black circle, then by Proposition 2 (see Section 3.2) a flux *maximising* connection can be made along the black line segment intersecting the two trajectories. □

We now consider a situation in which g has explicit t-dependence. Rather than artificially prescribing g, we will consider a g which is obtained by a natural advection process (more implications for such gs are examined in detail in Section 5).

Example 5 (*Time-Dependent Advected Weight Function*)**.** Consider the system

$$\left.\begin{aligned} \dot{x} &= x - x^2 \\ \dot{y} &= y^2 \end{aligned}\right\}, \tag{13}$$

and suppose $0 \leq t < 1$ to avoid finite-time blow-up issues. Fig. 4 displays the phase portrait of (13). Points in the regions $R = \{(x, y) : x > 1 \text{ and } y > 0\}$ and $L = \{(x, y) : x < 0 \text{ and } y < 0\}$ are the interesting regions for a flux extremising problem, since all other regions can be connected together along trajectories via the two fixed points at $(0, 0)$ and $(1, 0)$. Let $g(x, y, t)$ be the passively advected field generated from the initial condition $g(x, y, 0) = |y| + 1$. Then,

$$g(x, y, t) = \left|\frac{y}{1 + ty}\right| + 1 \tag{14}$$

since the y-coordinate evolves independently of x according to $y(t) = y(0)/(1 - y(0)t)$ and hence $y(0) = y(t)/(1 + ty(t))$. We restrict attention to the region R, in which $y > 0$, enabling the absolute value in (14) to be removed. Following Definition 7, we find

$$\kappa_g(x, y, t) = \frac{y^2}{(1 + ty)^2} + (1 - 2x + 2y)\left(\frac{(1 + t)y + 1}{1 + ty}\right)$$

and that the zero set of κ_g is given by

$$K_g(t) = \left\{(x, y) : x = \frac{y(t(2y + 1)(ty + y + 2) + 3(y + 1)) + 1}{2(ty + 1)(ty + y + 1)}\right\}$$

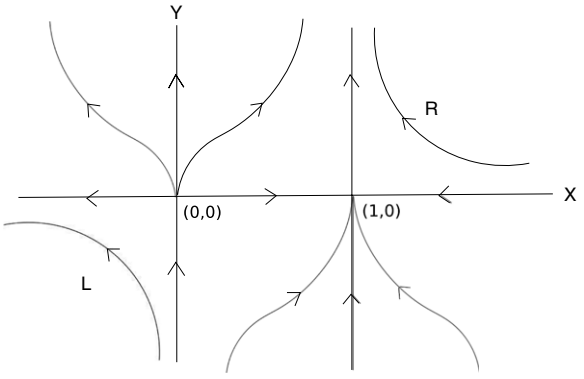

Fig. 4. The phase portrait of Example 5.

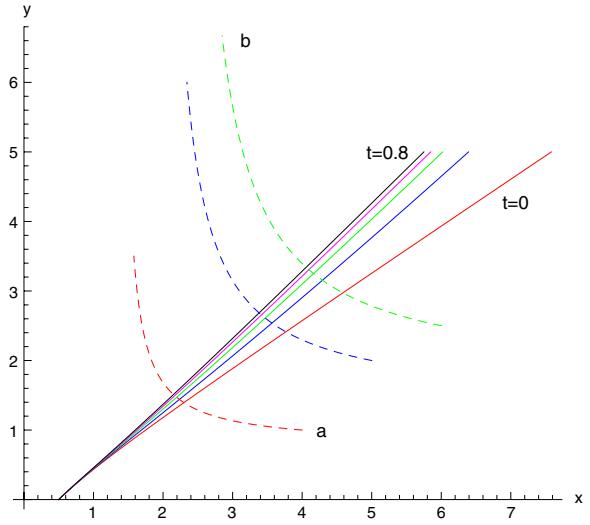

Fig. 5. The $K_g(t)$ sets (the almost straight solid curves) at five different times ($t = 0, 0.2, 0.4, 0.6, 0.8$), along with several trajectories (the dashed curves) of (13).

at each time t. These curves are indicated at several different times in Fig. 5 (the almost straight solid curves) along with several trajectories (the dashed curves) of (13). The value of $D_{\mathbf{f}}\kappa_g$ on $K_g(t)$ can be computed exactly, and takes the form of a rational function in y with coefficients which are polynomials in t. This is positive for values of y above a t-dependent threshold value, and evolves monotonically in t from 0.318254 at $t = 0$ to 0.332832 at $t = 1$.[4] Thus, if attempting to connect two points **a** and **b** in R as indicated in Fig. 5, one proceeds along the trajectories until intersecting the $K_g(t)$ curve corresponding to the appropriate time t, and makes the connection along that curve. □

3.2. Local absolute flux maximising curves

Obtaining an absolute flux maximising result analogous to Theorem 2 is clearly impossible, since the absolute flux across a curve can be made larger by simply making the curve longer and more contorted (in contrast to the signed flux, the absolute flux has a non-negative contribution at each point on the curve). Nevertheless, a "local maximising" result, exactly analogous to Proposition 1, is possible if restricting to a certain class of curves. The compressibility-decreasing subset $K_g^-(t)$ of $K_g(t)$ is defined by

$$K_g^-(t) := \left\{\mathbf{x} \in K_g(t) : \mathbf{f} \cdot \nabla \kappa_g(\mathbf{x}, t) < 0\right\} = \left\{\mathbf{x} \in K_g(t) : D_{\mathbf{f}}\kappa_g(\mathbf{x}, t) < 0\right\}, \tag{15}$$

and we hypothesise that $K_g(t)$ and $K_g^-(t)$ are one-dimensional, and that there exists a point in $I_{\mathbf{a}} \cap K_g^-(t)$ and a point in $I_{\mathbf{b}} \cap K_g^-(t)$ which can be connected by a piecewise C^1-smooth simple curve segment $\mathcal{C}_- \subseteq K_g^-(t) \subseteq K_g(t)$ of positive length

[4] The value at $t = 0$ is exactly expressible, but since all other values require numerical evaluation numerical values are given here.

contained in the interior of Ω. Suppose $\mathcal{C}_-$ is parametrised by $\mathbf{r}_-(p)$, where $0 \leq p \leq 1$, and $\mathbf{r}_-(0) \in I_{\mathbf{a}}$ and $\mathbf{r}_-(1) \in I_{\mathbf{b}}$. Define a non-degenerate fattening of $\mathcal{C}_-$ analogous to Definition 15, with $\mathcal{C}_+$ and $\mathbf{r}_+$ being replaced by $\mathcal{C}_-$ and $\mathbf{r}_-$ respectively.

Proposition 2 (*Absolute Flux-Maximising $\mathcal{C}_-$-Generated Curve*)**.** *Let S_T be a non-degenerate fattening set of $\mathcal{C}_-$. Then, for all $\mathcal{C}_-$-generated curves $\mathcal{C}_\tau \neq \mathcal{C}_-$ in S_T, $\mathcal{C}_-$ has the greatest absolute flux at time t, i.e.,*

$$F_g^a(\mathcal{C}_-, t) > F_g^a(\mathcal{C}_\tau, t).$$

Proof. See Appendix A.7. □

4. Degenerate situation in absolute flux optimisation

The previous sections outlined the possibility of obtaining curves which optimised the absolute flux in a certain sense: those curves, in comparison to "nearby" ones, represented a minimum (or maximum) of the flux. However, in a situation which is natural in fluid mechanics, the optimisation problem is degenerate in that for *all* curves of a certain class lying in a region, the absolute flux is identical. Let $\mathcal{C}_0$ be a simple curve segment of finite length lying in the interior of Ω, such that the flow across $\mathcal{C}_0$ is uni-directional.

Hypothesis 3 (*Weighted Incompressible Flow*)**.** The weighted compressibility $\kappa_g = 0$ on Ω at time t.

Theorem 3 (*Absolute Flux Degeneracy Under Weighted Incompressibility*)**.** *There exists a fattening set S_T of $\mathcal{C}_0$, such that the absolute flux across all $\mathcal{C}_0$-generated curves lying in S_T is identical.*

Proof. This is a straightforward result obtained by following the proof structure of Proposition 1 and obtaining a zero from the divergence theorem (Lemma 5). □

For the standard flux ($g = 1$) in incompressible flows ($\kappa_1 = 0$), this is a stationarity result in two-dimensional area-preserving flows, and is immediate from an easy application of the divergence theorem. MacKay's result of stationarity of algebraic (signed) flux in three-dimensional volume-preserving flows [27] is closely related.

5. Weighted flux

Our previous results indicate that for a weight function $g(\mathbf{x}, t)$, at each time instant, the location of $\kappa_g = 0$ (the set $K_g(t)$) is important in determining flux extremising curves. Knowing the temporal evolution of this set is therefore relevant. It is possible to characterise this evolution for some important choices of the weight $g(\mathbf{x}, t)$: that resulting from the evolution by the flow of an initial distribution $g(\mathbf{x}, 0)$. There are two main ways this can be done:

1. Consider $g(\mathbf{x}, 0)$ as a *density*: If g is a density, one may use g to naturally model non-equilibrium concentration of passive tracers or chemicals in the domain Ω, and to calculate curves over which the tracer or chemical flux is minimal/maximal.
2. Consider $g(\mathbf{x}, 0)$ as a *conserved function*: In this case we think of g as a quantity which is advected by the flow and each particle retains its g value over time. For example, if g is the vorticity or potential vorticity of an unsteady flow, it is conserved by fluid particles (i.e., advected by the flow), in which case we are also able to make statements regarding the evolution of zero-level sets of κ_g.

5.1. The weight g is a density

Suppose that g is a density, which also includes the possibility of g being a concentration of a chemical in the flow. It can be shown that $\kappa_g = \nabla \cdot (\mathbf{f}g) = 0$ if and only if g is an *invariant density* of the flow; see for example, Theorem 7.8.2 [24]. This result is known as Liouville's theorem.

This choice of g (g is preserved by the flow) is particularly interesting from a dynamical point of view. Preservation of the *density* g by the flow can be written in terms of the associated *probability measure* defined by $\mu_g(B) = \int_B g \, dm_2$, where B is a (Borel) measurable subset of Ω. Then $g = d\mu_g/dm_2$, the Radon–Nikodym derivative of μ_g. The probability measure μ_g is said to be *flow-invariant* or an *invariant probability measure* if $\mu_g = \mu_g \circ \phi(\cdot, -t)$ for all $t \in \mathbb{R}$; that is, μ_g is equal to its push-forward under the flow for all t. We say that the density g is *preserved by the flow* or an *invariant density* if μ_g is flow-invariant or an invariant probability measure. If μ_g is additionally *ergodic*,[5] by Birkhoff's ergodic theorem (see e.g. Walters [41][6]) one has for $h \in L^1(\Omega, \mu_g)$

$$\lim_{t\to\infty} \frac{1}{t} \int_0^t h(\phi(\mathbf{x}, \tau)) d\tau = \int_\Omega h(\mathbf{x}) \, d\mu_g(\mathbf{x}) \quad \text{for } \mu_g \text{ almost-all } \mathbf{x}. \tag{16}$$

[5] The probability measure μ_g is ergodic if the only invariant sets have full or trivial μ_g-measure; i.e., if $B \subset \Omega$ satisfies $\phi(B, -t) = B$ for all $t \in \mathbb{R}$, then $\mu_g(B) = 0$ or 1.

[6] The discrete time version of the Birkhoff theorem stated in [41] is easily converted to a continuous time version by applying the discrete time version to $\phi(\mathbf{x}, 1)$, the time-1 flow map, and the function $\tilde{h}(\mathbf{x}) := \int_0^1 h(\phi(\mathbf{x}, t)) \, dt$.

In particular, if $B \subset \Omega$, setting $h = \chi_B$ one has

$$\lim_{t\to\infty} \frac{1}{t}\int_0^t \chi_B(\phi(\mathbf{x},\tau))d\tau = \int_\Omega \chi_B(\mathbf{x})\, d\mu_g(\mathbf{x}) = \mu_g(B) \quad \text{for } \mu_g \text{ almost-all } \mathbf{x}. \tag{17}$$

Eq. (17) states that the frequency with which trajectories visit a set $B \subset \Omega$ is given by the measure of B, $\mu_g(B)$. Thus, the choice of weighting g that leads to the degenerate flux optimisation setting is the weighting given by the distribution of long trajectories of the flow. In the specific case of area-preserving flow, this distribution is uniform and $g \equiv 1$.

The interesting situation is when g is not preserved by the flow, as occurs when the concentration represented by g is not in equilibrium with the flow. By [24, pp. 211–213] and the definition of κ_g in (7), the density g is advected according to

$$\frac{\partial g}{\partial t} = -\nabla\cdot(\mathbf{f}g) \tag{18}$$

(the "continuity equation"). Observe from (18) that $\kappa_g = -\partial g/\partial t$, which gives an alternative representation of the flux extremising curves which are associated with $\kappa_g = 0$. This evolution of g also allows one to determine the time-evolution of the zero-level-sets of κ_g, within which local flux minimising curves must lie.

Theorem 4 (*Evolution for a Density*)**.** *Let Ω be compact, $g(\mathbf{x},0)$ be a C^2 initial density with compact support and let $g(\mathbf{x},t)$ represent the push-forward of $g(\mathbf{x},0)$ after a time $t \geq 0$ under the flow $\phi(\cdot,t)$ generated by (1). Then $\kappa_g(\mathbf{x},t)$ evolves as a push-forward of a (scaled) signed density (i.e. it satisfies $\partial\kappa_g/\partial t = -\nabla\cdot(\kappa_g\mathbf{f})$) and the zero-level-sets of κ_g evolve by advection under ϕ; that is,*

$$\{\mathbf{x}\in\Omega : \kappa_g(\mathbf{x},t) = 0\} = \phi(\{\mathbf{x}\in\Omega : \kappa_g(\mathbf{x},0) = 0\}, t).$$

Proof. Using (18),

$$\frac{\partial\kappa_g}{\partial t} = \frac{\partial(\nabla\cdot(\mathbf{f}g))}{\partial t} = \nabla\cdot\left(\frac{\partial(\mathbf{f}g)}{\partial t}\right) = \nabla\cdot\left(\frac{\partial g}{\partial t}\mathbf{f}\right) = -\nabla\cdot(\kappa_g\mathbf{f}). \tag{19}$$

The *Perron–Frobenius operator* pushes forward densities with the flow map ϕ and is defined by

$$\mathcal{P}^t h(\mathbf{x}) = h\circ\phi(\mathbf{x},-t)/|\det D\phi(\phi(\mathbf{x},-t),t)|, \quad h\in L^1(\Omega). \tag{20}$$

The operators $\mathcal{P}^t$ form a C^0 semigroup of bounded linear operators on L^1, and by Theorem 2.6 [32] are the only such semigroup with generator (or *infinitesimal operator*) $-\nabla\cdot(\mathbf{f}h)$ (cf. [24]). Therefore, the function $\kappa_g(\mathbf{x},t) := \mathcal{P}^t\kappa_g(\mathbf{x},0)$ is the unique bounded C^0 semigroup solution of (19).

Now

$$\begin{aligned}\{\mathbf{x}\in\Omega : \kappa_g(\mathbf{x},t) = 0\} &= \{\mathbf{x}\in\Omega : \mathcal{P}^t\kappa_g(\mathbf{x},0) = 0\}\\ &= \{\mathbf{x}\in\Omega : \kappa_g(\phi(\mathbf{x},-t),0) = 0\}\\ &= \{\phi(\mathbf{x},t)\in\Omega : \kappa_g(\mathbf{x},0) = 0\}\\ &= \phi(\{\mathbf{x}\in\Omega : \kappa_g(\mathbf{x},0) = 0\}, t),\end{aligned}$$

where the second equality follows from (20) since $0 < |\det D\phi| < \infty$ and Ω is compact. □

If $g(\mathbf{x},0)$ is an *invariant* density, then $\partial g/\partial t = -\kappa_g = 0$ and so the field κ_g is unchanging (and identically equal to zero).

Theorem 5. *With the setting and notation of Theorem 4, one has $K_g^+(t) = \phi(K_g^+(0),t)$ and $K_g^-(t) = \phi(K_g^-(0),t)$ for $t \geq 0$. Thus, locally flux minimising curves are advected by the flow ϕ.*

Proof. First, we calculate:

$$\begin{aligned}\frac{\partial(D_{\mathbf{f}}\kappa_g)}{\partial t} &= \frac{\partial(\mathbf{f}\cdot\nabla(\nabla\cdot(\mathbf{f}g)))}{\partial t}\\ &= \mathbf{f}\cdot\nabla(\nabla\cdot(\mathbf{f}\partial g/\partial t))\\ &= -\mathbf{f}\cdot\nabla(\nabla\cdot(\mathbf{f}\kappa_g)) \quad \text{(cf. proof of Theorem 4)}\\ &= -\mathbf{f}\cdot\nabla((\nabla\cdot\mathbf{f})\kappa_g + \mathbf{f}\cdot\nabla\kappa_g)\\ &= -\mathbf{f}\cdot(\nabla(\nabla\cdot\mathbf{f})\kappa_g + (\nabla\cdot\mathbf{f})\nabla\kappa_g) - \mathbf{f}\cdot\nabla(\mathbf{f}\cdot\nabla\kappa_g)\\ &= -\mathbf{f}\cdot\nabla(\nabla\cdot\mathbf{f})\kappa_g - (\nabla\cdot\mathbf{f})(\mathbf{f}\cdot\nabla\kappa_g) - \mathbf{f}\cdot\nabla(\mathbf{f}\cdot\nabla\kappa_g)\\ &= -\mathbf{f}\cdot\nabla(\nabla\cdot\mathbf{f})\kappa_g - \nabla\cdot\big((\mathbf{f}\cdot\nabla\kappa_g)\mathbf{f}\big)\\ &= -\mathbf{f}\cdot\nabla(\nabla\cdot\mathbf{f})\kappa_g - \nabla\cdot(\mathbf{f}\,D_{\mathbf{f}}\kappa_g)\\ &= -(D_{\mathbf{f}}\kappa_1)\kappa_g - \nabla\cdot\big(\mathbf{f}D_{\mathbf{f}}\kappa_g\big).\end{aligned}$$

As argued in the proof of Theorem 4, *if* $\partial(D_{\mathbf{f}}\kappa_g)/\partial t = -\nabla\cdot(\mathbf{f}D_{\mathbf{f}}\kappa_g)$ then the function $D_{\mathbf{f}}\kappa_g$ evolves *as a signed density* under the flow. In particular, over a finite flow time, as in the proof of 4, zero-level-sets of $D_{\mathbf{f}}\kappa_g$ would be advected by ϕ, and furthermore, the positive and negative supports of $D_{\mathbf{f}}\kappa_g$ would also be advected by ϕ. There is, however, an additional term $-(D_{\mathbf{f}}\kappa_1)\kappa_g$, but for $\mathbf{x}\in K_g(t)$, $\kappa_g(\mathbf{x},t)=0$ and this term vanishes. Thus, on $K_g(t)$, the positive and negative supports of $D_{\mathbf{f}}\kappa_g$ (namely $K_g^+(t)$ and $K_g^-(t)$) are advected by ϕ. Repeating the argument from the proof of Theorem 4, one therefore has

$$\begin{aligned}
\{\mathbf{x}\in K_g^+(t)\} &= \{\mathbf{x}\in\Omega : \kappa_g(\mathbf{x},t)=0, D_{\mathbf{f}}\kappa_g(\mathbf{x},t)>0\}\\
&= \{\mathbf{x}\in\Omega : \mathcal{P}^t\kappa_g(\mathbf{x},0)=0, \mathcal{P}^t(D_{\mathbf{f}}\kappa_g)(\mathbf{x},0)>0\} \qquad (21)\\
&= \{\mathbf{x}\in\Omega : \kappa_g(\phi(\mathbf{x},-t),0)=0, D_{\mathbf{f}}\kappa_g(\phi(\mathbf{x},-t),0)>0\} \qquad (22)\\
&= \{\phi(\mathbf{x},t)\in\Omega : \kappa_g(\mathbf{x},0)=0, D_{\mathbf{f}}\kappa_g(\mathbf{x},0)>0\}\\
&= \phi(\{\mathbf{x}\in\Omega : \kappa_g(\mathbf{x},0)=0, D_{\mathbf{f}}\kappa_g(\mathbf{x},0)>0\},t)\\
&= \phi(K_g^+(0),t),
\end{aligned}$$

where (21) follows by Theorem 4 and the arguments above, and (22) follows from (20), the fact that $0<|\det D\phi|<\infty$, and compactness of Ω. The result for $K_g^-(t)$ follows identically. □

Example 6 (Example 4 *Cont…*)**.** We demonstrate Theorems 4 and 5 by calculating the location of flux minimal curves in two ways. Firstly, by beginning with a uniform weight $g\equiv 1$ at time 0, (as in Example 4) and then numerically estimating $g(\cdot,t)$ for $t=0.05$. We consider g as a density and numerically estimate $g(\cdot,t)$ by discretising a domain $[-6,6]\times[-6,6]$ into 360×360 square grid cells and integrating forward 100 uniformly distributed test points within each grid cell. The images of these test points are then used to create a histogram at time $t=0.05$ on the grid cells restricted to the square $[-4,4]\times[-4,4]$ (we use the larger initial domain $[-6,6]\times[-6,6]$ to ensure it contains the preimage of $[-4,4]\times[-4,4]$). We then apply an interpolation to smooth the resulting histogram (this removes sampling errors due to a finite number of test points), and then numerically compute κ_g and $D_{\mathbf{f}}\kappa_g$ by central difference methods. The resulting estimates of the zero-level-sets of κ_g and $D_{\mathbf{f}}\kappa_g$ at time $t=0.05$ are shown as zero-level contours in Figs. 6 and 7. Secondly (and with considerably less effort), utilising Theorems 4 and 5 we numerically advect the zero-level-sets of κ_g and $D_{\mathbf{f}}\kappa_g$ determined in Example 4 at $t=0$. These are shown as curves of small circles in Figs. 6 and 7. □

5.2. The weight g is a conserved function

Now suppose g is a function which is conserved by fluid particles under the flow (1). This implies that g's material derivative is zero, that is

$$0=\frac{D}{Dt}g := \frac{\partial g}{\partial t}+\mathbf{f}\cdot\nabla g = \frac{\partial g}{\partial t}+\nabla\cdot(\mathbf{f}g)-g\,(\nabla\cdot\mathbf{f}) = \frac{\partial g}{\partial t}+\kappa_g-g\,\kappa_1 \qquad (23)$$

An equivalent viewpoint is that the function g is advected forward $t\geq 0$ time units by $U_t'g(\mathbf{x}) := g\circ\phi(\mathbf{x},-t)$. Following [24, pp. 210–211], $\{U_t'\}_{t\geq 0}$ is a continuous semigroup on a subspace of C^1, compactly supported, L^∞ functions. Taking a time derivative of U_t' as $t\to 0$, one obtains the infinitesimal operator $\mathcal{K}'g := -\mathbf{f}\cdot\nabla g$ that generates the semigroup $\{U_t'\}_{t\geq 0}$. One has $g(\mathbf{x},t)=U_t'g(\mathbf{x})$ satisfying $\partial g/\partial t=-\mathbf{f}\cdot\nabla g$ (as in (23)). The operator $U_t := g\circ\phi(\mathbf{x},t)$ is commonly known as the *Koopman operator*, and for $t\geq 0$ is a pull-back; thus we consider U_t', which is merely the "backward time" Koopman operator, and amounts to a push-forward for $t\geq 0$.

For this situation, the important sets $K_g(t)$ and $K_g^\pm(t)$ do not evolve cleanly with the flow as in Section 5.1. For purposes of evolution, the term that plays the role that κ_g took in Section 5.1 is

$$\kappa_g-g\kappa_1 = D_{\mathbf{f}}g = -\frac{\partial g}{\partial t} \qquad (24)$$

in which the equalities are because of the definition of κ_g in (7) and (23) respectively. We define

$$\tilde{K}_g(t) := \left\{\mathbf{x}\in\Omega : \kappa_g(\mathbf{x},t)-g(\mathbf{x},t)\kappa_1(\mathbf{x},t)=0\right\}$$

along with its subsets

$$\tilde{K}_g^\pm(t) := \left\{\mathbf{x}\in\tilde{K}_g(t) : D_{\mathbf{f}}\left[\kappa_g(\mathbf{x},t)-g(\mathbf{x},t)\kappa_1(\mathbf{x},t)\right]\gtrless 0\right\}.$$

Theorem 6 (*Evolution for An Advected Function*)**.** *If g is advected by the flow, the quantity $\kappa_g-g\kappa_1$ is conserved by fluid particles. Thus, $\tilde{K}_g(t)=\phi\left(\tilde{K}_g(0),t\right)$. Moreover, $D_{\mathbf{f}}\left(\kappa_g-g\kappa_1\right)$ is conserved by fluid particles, and hence $\tilde{K}_g^+(t)=\phi\left(\tilde{K}_g^+(0),t\right)$ and $\tilde{K}_g^-(t)=\phi\left(\tilde{K}_g^-(0),t\right)$.*

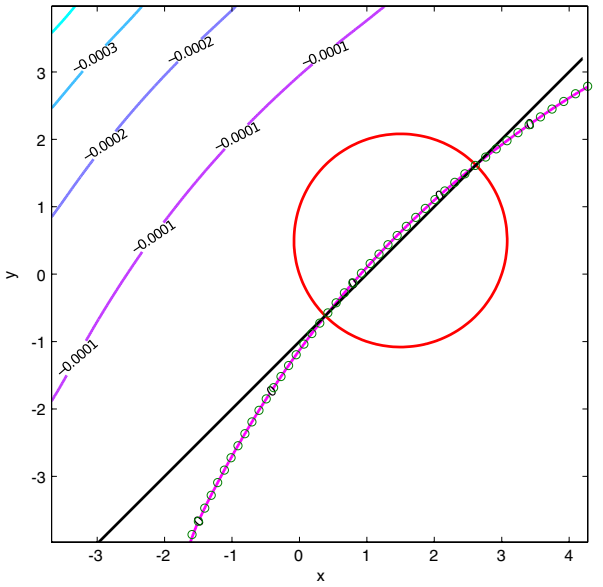

Fig. 6. (Contours of $\kappa_g(0.05)$): The set $\{\kappa_g(0) = 0\}$ (the line $y = x - 1$) as calculated in Example 4 is shown as a solid black line. The set $\{D_{\mathbf{f}}\kappa_g(0) = 0\}$ from Example 4 is the red circle. The contours of $\kappa_g(0.05)$ are as indicated. Note that the zero contour is perfectly covered by small circles; the curve indicated by the small circles is the result of directly advecting the solid black line from time $t = 0$ to $t = 0.05$ and demonstrates the conclusion of Theorem 4. (For interpretation of the references to colour in this figure legend, the reader is referred to the web version of this article.)

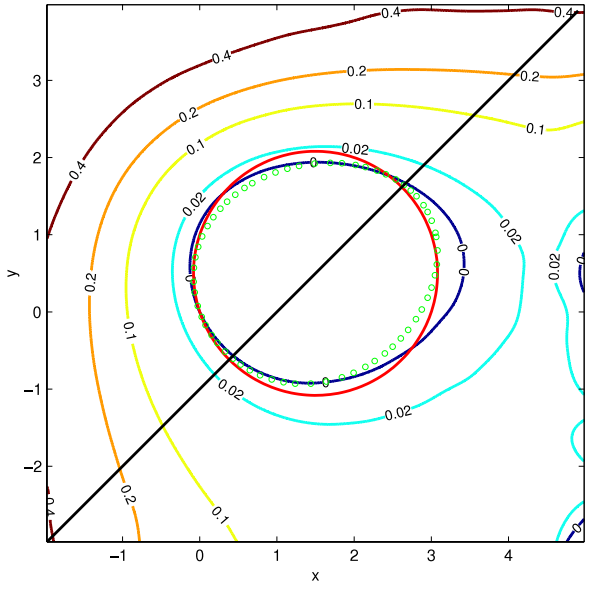

Fig. 7. (Contours of $D_{\mathbf{f}}\kappa_g(0.05)$): The set $\{\kappa_g(0) = 0\}$ (the line $y = x - 1$) as calculated in Example 4 is shown as a solid black line. The set $\{D_{\mathbf{f}}\kappa_g(0) = 0\}$ from Example 4 is the red circle. The contours of $D_{\mathbf{f}}\kappa_g(0.05)$ are as indicated. The curve indicated by the small green circles is the result of directly advecting the red circle from time $t = 0$ to $t = 0.05$. The graphical interpretation of Theorem 5 is that the interior (resp. exterior) of the closed zero-level contour of this figure intersected with the zero-level contour in Fig. 6 coincides with the interior (resp. exterior) of the closed curve of green circles in this figure intersected with the curve of circles in Fig. 6. (For interpretation of the references to colour in this figure legend, the reader is referred to the web version of this article.)

Proof. Note that

$$\frac{\partial \kappa_g}{\partial t} = \frac{\partial}{\partial t}\left[\nabla \cdot (g\mathbf{f})\right] = \nabla \cdot \left[\mathbf{f}\frac{\partial g}{\partial t}\right] = \nabla \cdot \left[\mathbf{f}\left(g\kappa_1 - \kappa_g\right)\right]$$

by using (23). Thus

$$\begin{aligned}\frac{\partial \kappa_g}{\partial t} &= (\nabla\cdot\mathbf{f})\, g\kappa_1 + \mathbf{f}\cdot\nabla(g\kappa_1) - \nabla\cdot\left(\mathbf{f}\kappa_g\right)\\ &= g\kappa_1^2 + \mathbf{f}\cdot\nabla(g\kappa_1) - (\nabla\cdot\mathbf{f})\,\kappa_g - \mathbf{f}\cdot\left(\nabla\kappa_g\right)\\ &= \kappa_1\left(g\kappa_1-\kappa_g\right) + \mathbf{f}\cdot\nabla(g\kappa_1) - \mathbf{f}\cdot\nabla\kappa_g,\end{aligned}$$

and hence

$$\begin{aligned}\frac{D}{Dt}\left(\kappa_g\right) &= \frac{\partial\kappa_g}{\partial t} + \mathbf{f}\cdot\nabla\kappa_g = \kappa_1\left(g\kappa_1-\kappa_g\right) + \mathbf{f}\cdot\nabla(g\kappa_1)\\ &= \kappa_1\left(g\kappa_1-\kappa_g\right) + \frac{D}{Dt}(g\kappa_1) - \frac{\partial}{\partial t}(g\kappa_1)\\ &= \kappa_1\left(g\kappa_1-\kappa_g\right) + \frac{D}{Dt}(g\kappa_1) - \kappa_1\frac{\partial g}{\partial t}\\ &= \frac{D}{Dt}(g\kappa_1)\end{aligned}$$

since κ_1 is time-independent, and by utilising (23) in the final step. Thus, $D/Dt\left(\kappa_g - g\kappa_1\right) = 0$, that is, the quantity $\kappa_g - g\kappa_1$ is conserved by fluid particles. This implies that the zero-level sets of this quantity are advected by the flow ϕ. Now we compute

$$\begin{aligned}\frac{D}{Dt}\left[D_{\mathbf{f}}\left(\kappa_g - g\kappa_1\right)\right] &= \frac{D}{Dt}\left[\mathbf{f}\cdot\nabla\left(\kappa_g - g\kappa_1\right)\right]\\ &= \frac{\partial}{\partial t}\left[\mathbf{f}\cdot\nabla\left(\kappa_g - g\kappa_1\right)\right] + \mathbf{f}\cdot\nabla\left[\mathbf{f}\cdot\nabla\left(\kappa_g - g\kappa_1\right)\right]\\ &= \mathbf{f}\cdot\nabla\left[\frac{\partial}{\partial t}\left(\kappa_g - g\kappa_1\right)\right] + \mathbf{f}\cdot\nabla\left[\mathbf{f}\cdot\nabla\left(\kappa_g - g\kappa_1\right)\right]\\ &= D_{\mathbf{f}}\left[\frac{\partial}{\partial t}\left(\kappa_g - g\kappa_1\right) + \mathbf{f}\cdot\nabla\left(\kappa_g - g\kappa_1\right)\right]\\ &= D_{\mathbf{f}}\left[\frac{D}{Dt}\left(\kappa_g - g\kappa_1\right)\right]\\ &= 0.\end{aligned}$$

Since this implies that $D_{\mathbf{f}}\left(\kappa_g - g\kappa_1\right)$ is conserved by the flow, parts of the zero level set of $\kappa_g - g\kappa_1$ at time zero at which $D_{\mathbf{f}}$ were positive would continue to have the same positive value once evolved by the flow ϕ, and a similar result holds for its subsets where $D_{\mathbf{f}}$ were negative. □

We remark that the level sets which evolve with the flow are here associated with $\kappa_g - g\kappa_1$, which is equal to $-\partial g/\partial t$. In the case in which g were a density as addressed in Section 5.1, the quantity of interest was κ_g, which was *also* equal to $-\partial g/\partial t$. Hence, in both of the advected situations the zero-level sets of $\partial g/\partial t$ are advected by the flow, and also preserve the quantity $D_{\mathbf{f}}(\partial g/\partial t)$ which is associated with the flow directionality across the curve.

Example 7 (*Time-Dependent Advected g (Cont.)*)**.** We continue Example 5, once again considering the region R. Here, $\kappa_1(x,y) = 1-2x+2y$, and straightforward algebra leads to $\kappa_g - g\kappa_1 = y^2/(1+ty)^2$. This quantity is obviously conserved since it can be written as $(g(x,y,t)-1)^2$, and g is conserved by the flow. Moreover, $D_{\mathbf{f}}\left(\kappa_g - g\kappa_1\right) = 2y^3/(1+ty)^3 = 2\left(g(x,y,t)-1\right)^3$, which is therefore also conserved. This verifies Theorem 6. An alternative approach would be to compute $\partial g/\partial t = -y^2/(1+ty)^2$ in R, from which identical conclusions could be drawn. Note that in this case neither κ_g nor $D_{\mathbf{f}}\kappa_g$ is conserved by the flow, and thus flux extremising curves are not carried along with the flow. □

While Theorem 6 tells us that flux extremising curves are *not* advected by the flow in general, in one physically relevant situation, they are:

Corollary 1. *Suppose the flow (1) is incompressible; i.e., $\kappa_1 = 0$. If g is advected by the flow, then κ_g and $D_{\mathbf{f}}\kappa_g$ are both conserved by fluid particles. Thus, $K_g(t) = \phi\left(K_g(0),t\right)$ and $K_g^{\pm}(t) = \phi\left(K_g^{\pm}(0),t\right)$.*

Proof. If $\kappa_1 = 0$, then the definitions for $\tilde{K}_g$ and $\tilde{K}_g^{\pm}$ collapse to the definitions for K_g and $K_g^{\pm}$ respectively, and the corollary follows. □

Example 8 (*Vorticity Flux*)**.** Consider two-dimensional inviscid, incompressible fluid motion. In this case, there exists a streamfunction $\psi(x,y)$ such that the velocity field is $\mathbf{f} = \left(\psi_y, -\psi_x\right)$. Let $g = \nabla^2\psi$, which represents the vorticity (curl)

of the velocity field **f**. Thus, g is an active scalar in this instance, and the relevant flux here is the *vorticity flux*, measuring the amount of vorticity (modulated by the fluid area) transferred across a curve in unit time. The vorticity equation [1, e.g.] guarantees that g is conserved along flow trajectories, and hence from Corollary 1 the level sets of

$$\kappa_g = \psi_y \left(\nabla^2\psi\right)_x - \psi_x \left(\nabla^2\psi\right)_y = D_{\mathbf{f}} \left(\nabla^2\psi\right)$$

are advected by the flow. Here, κ_g has several possible interpretations: it is the flow derivative of the vorticity, and also the Poisson bracket between the vorticity $\nabla^2\psi$ and the streamfunction ψ. Thus, zero-level sets of κ_g are carried along with the flow. Moreover, the subsets of this zero-level set at time zero at which $D_{\mathbf{f}}\kappa_g > 0$ preserve the same value for $D_{\mathbf{f}}\kappa_g$ as the flow evolves, and thus locally flux-minimising curves are advected by the flow. Since $\kappa_1 = 0$ under incompressibility, (23) implies that κ_g is zero throughout the flow domain, and thus there is degeneracy of vorticity flux-extremising curves by Theorem 3. This is of course closely related to the classical Stokes' theorem representation of Kelvin's circulation theorem [1, e.g.]. □

Example 9 (*Rossby Wave and Potential Vorticity Flux*)**.** An approximation used for oceanic flows is that of the barotropic β-plane [33], in which incompressible inviscid flow with streamfunction $\psi(x, y, t)$ generates a potential vorticity field $q(x, y, t) = \nabla^2\psi + \beta y$ (where β is a constant related to the latitude near which the motion occurs) which is conserved by the flow. That is, its material derivative $Dq/Dt = \partial q/\partial t + \mathbf{f} \cdot \nabla q = 0$. An exact solution to this nonlinear PDE in ψ is a Rossby wave solution [34] $\psi(x, y, t) = \gamma \sin[k(x - ct)] \sin[ly]$ for wavenumbers (k, l) and arbitrary constant γ, in which the travelling wavespeed c satisfies $c(k^2 + l^2) = -\beta$. For $\gamma k(k^2 + l^2) > \beta$, this forms an idealised model for eastward flowing meandering oceanic jets such as the Gulf Stream. Setting $(X, Y) = (x - ct, y)$ to be coordinates in a frame travelling with the wave enables the removal of the explicit time-dependence, and the flow to be written in terms of the moving streamfunction $\Psi(X, Y) = \psi(x, y) + cy$ such that its velocity field is $\mathbf{F}(X, Y) = (-\Psi_Y, \Psi_X)$. The potential vorticity in the moving frame, $Q(X, Y)$ can be seen to satisfy $-(k^2 + l^2)\Psi$. In this moving frame,

$$\kappa_g = \Psi_Y Q_X - \Psi_X Q_Y = -\left(k^2 + l^2\right)\left[\Psi_Y \Psi_X - \Psi_X \Psi_Y\right] = 0.$$

(Alternatively, since g is time-independent in the moving frame, $-\partial g/\partial t = 0$.) Theorem 1 therefore tells us that in the moving frame, there is degeneracy of potential vorticity flux extremising curves. □

6. Concluding remarks

In this article, we have addressed the issue of determining absolute flux optimising curves connecting points on two trajectories in two-dimensional autonomous flows in which the flux definition includes for the possibility of a temporally and spatially varying weight. We considered the possibility of a bounded or unbounded domain, and were able to quantify locally and globally flux optimising curves at each instance in time. The quantity which governed our ability to identify these curves was the divergence of the vector field which is formed by taking the product of the weight and the flow velocity. The inclusion of a weight function permitted us to account for naturally advected quantities such as a density (e.g., a chemical concentration) or a materially-conserved quantity (e.g., a vorticity field); two special situations which were addressed in more detail in Section 5, in which we showed that in these cases the optimising curves of interest are usually advected by the flow.

Acknowledgments

SB acknowledges partial support from the Simons Foundation (grant #236923), and from MASCOS which sponsored his visit to UNSW. GF acknowledges partial support from the ARC Centre of Excellence in Mathematics and Statistics. NS acknowledges partial support from MASCOS while at UNSW, and from MURI-ONR while at UNC.

Appendix. Proofs

A.1. Preliminary lemmas

We state some elementary lemmas which are useful in the subsequent proofs. The proofs will be skipped.

Lemma 4 (*Forward–Backwards Flux*)**.** *Calculating the signed flux along a curve with the direction along the curve and the normal direction both reversed, results in negative the original flux.*

Lemma 5 (*Divergence Theorem*)**.** *Let $\mathcal{C}$ be a simple, closed, piecewise C^1 curve lying in Ω, parametrised by $\mathbf{r}(p)$ with p increasing in the clockwise direction. If S is the area enclosed by $\mathcal{C}$ and if m_2 is two-dimensional Lebesgue measure, then*

$$F_g^S(\mathcal{C}) = \iint_S \kappa_g \, \mathrm{d}m_2.$$

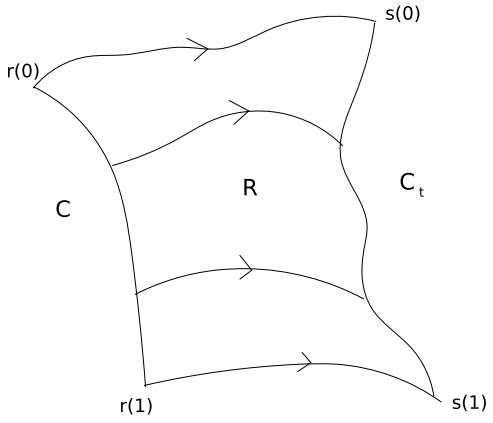

Fig. 8. Figure for Lemma 1 in which $\mathcal{C} \in K^p$ and $\mathcal{C}_\tau$ is in a positive fattening set.

A.2. Proof of Lemma 1 (one-sided flux optimisation)

Suppose that $\mathcal{C}$ is parametrised by the piecewise C^1 function $\mathbf{r}(p)$ where $p \in [0, 1]$. Consider first the case where $\mathcal{C} \in K_g^p$, and where $\mathcal{C}_\tau$ lies in a permissible positive fattening set of $\mathcal{C}$. Thus, $\mathcal{C}_\tau$ is associated with a piecewise C^1 function $\tau > 0$ on $\mathcal{C}$, which shall be (with an abuse of notation) considered a function on $p \in [0, 1]$. Since in a permissible fattening set of $\mathcal{C}$, each point of $\mathcal{C}_\tau$ has a flow in the same direction as the corresponding point on $\mathcal{C}$, and thus the flow on $\mathcal{C}_\tau$ is also unidirectional. Moreover, $\mathcal{C}_\tau$ is parametrised by $\mathbf{s}(p) = \phi(\mathbf{r}(p), \tau(p))$. Let R be the region bounded by $\mathcal{C}$, $\mathcal{C}_\tau$ and the trajectory segments $\{\phi(\mathbf{r}(0), t) : t \in [0, \tau(0)]\}$ and $\{\phi(\mathbf{r}(1), t) : t \in [0, \tau(1)]\}$ emanating from the ends of $\mathcal{C}$. See Fig. 8. Now, since the point flux across any point along the top and bottom trajectory boundaries is zero, the signed flux around the anti-clockwise closed loop around R in Fig. 8 is given by $F_g^s(\mathcal{C}, t) - F_g^s(C_\tau, t)$, in which we adopt the convention that we proceed along each curve in the positive direction of the parameter p. However, for the situation pictured in Fig. 8, $F_g^s = F_g^a$ for both $\mathcal{C}$ and $\mathcal{C}_\tau$, since the flux is in the leftwards direction in each case when traversing each curve in the direction of increasing p. Thus, the signed flux around the closed loop enclosing R is $F_g^a(\mathcal{C}, t) - F_g^a(C_\tau, t)$. Applying the divergence theorem (Lemma 5) and realising that the outward pointing normal is in the negative direction of the point flux,

$$F_g^a(\mathcal{C}, t) - F_g^a(C_\tau, t) = -\int_R \kappa_g \, \mathrm{d}m_2 < 0$$

since $\kappa_g > 0$ in K_g^p. Thus, $F_g^a(\mathcal{C}, t) < F_g^a(\mathcal{C}_\tau, t)$, as needed. This same result remains valid if the parametrisation on $\mathcal{C}$ is reversed (with the signed fluxes acquiring negative signs from those in Fig. 8), since the absolute flux does not change when traversing a curve in the reverse direction.

Proofs of the other three statements in Lemma 1 are exactly analogous, and will be skipped. □

A.3. Proof of Lemma 2 (uni-directional flux)

There can be no fixed points on $\mathcal{C}_+$ by the definition of K_g^+ (12), since $\mathbf{f} \cdot \nabla\kappa_g > 0$ on $\mathcal{C}_+$, it must be true that $\mathbf{f} \neq \mathbf{0}$ and $\nabla\kappa_g \neq \mathbf{0}$ on $\mathcal{C}_+$. Moreover, $\nabla\kappa_g$ is normal to $\mathcal{C}_+$ since $\mathcal{C}_+ \subset K_g$. Let $\mathbf{r}_+(p)$ parametrise $\mathcal{C}_+$. Now from Definition 4, $L_1(\mathbf{r}_+(p)) = \mathbf{f}(\mathbf{r}_+(p)) \cdot J\mathbf{r}_+'(p)$. Consider a point on $\mathcal{C}_+$ at which $\mathbf{r}_+'(p)$ is defined. It is not clear whether $L_1 > 0$ or $L_1 < 0$ here, because of the ambiguity in determining whether $J\mathbf{r}_+'(p)$ is in the direction of $\nabla\kappa_g$ or $-\nabla\kappa_g$.

Suppose first that the flow direction along $I_\mathbf{a}$ in Fig. 2 near the point at which $I_\mathbf{a}$ intersects $\mathcal{C}_+$ is from left to right; that is, that $L_1(\mathbf{r}_+(0)) < 0$. Then the flow across $\mathcal{C}_+$ near to $\mathbf{r}_+(0)$ must also be left to right by the rectification theorem (see for example [4]), and by continuity $L_1(\mathbf{r}_+(p))$ continues to be negative for small p. Now, by definition (12), it is necessary that $\nabla\kappa_g$ also point to the right on $\mathcal{C}_+$. As one progresses upwards along $\mathcal{C}_+$, $\nabla\kappa_g$ must continue to point from the left to the right, since $\mathcal{C}_+$ is part of a level set of κ_g, and such a reversal is only possible if going across a point at which $\nabla\kappa_g = \mathbf{0}$, which cannot lie on $\mathcal{C}_+$ by the definition (12). Thus, $\nabla\kappa_g$ will continue to point from left to right as one progresses upwards along $\mathcal{C}_+$ in Fig. 2. But since $\mathcal{C}_+$ lies on K_g^+, this ensures that $\mathbf{f}$ must also point from left to right on $\mathcal{C}_+$. This is true all the way up to $\mathbf{r}_+(1)$, and thus the flow along the integral set $I_\mathbf{b}$ is also from left to right.

The above argument works similarly if the flow along $I_\mathbf{a}$ is from right to left, that is, if $L_1(\mathbf{r}_+(p)) > 0$. In this case, the flow across $\mathcal{C}_+$, $\nabla\kappa_g$ on $\mathcal{C}_+$, and the flow along $I_\mathbf{b}$ must *all* point from right to left as well. Thus, the flow across $\mathcal{C}_+$ is uni-directional, i.e., the point flux is sign definite. □

A.4. Proof of Lemma 3 (existence of non-degenerate fattening set)

Condition (a) of the non-degeneracy definition (that the flow across $\mathcal{C}_\tau$ is in the same direction as that across $\mathcal{C}_+$) is true almost by definition. The rectification theorem [4] ensures the presence of a "flow-box" in the vicinity of each point on $\mathcal{C}_+$,

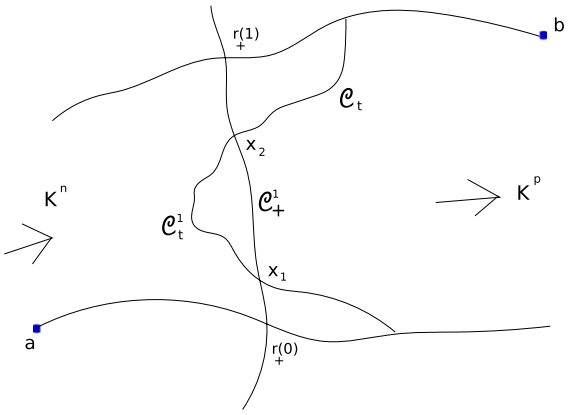

Fig. 9. Flux-minimising for $\mathcal{C}_+$-generated curves.

in which the flow is diffeomorphic to that of the two-dimensional system $\dot{x} = 1, \dot{y} = 0$. By following the flow from a point $\mathbf{r}_+(p)$ on $\mathcal{C}_+$ along a trajectory fibre, one arrives at a point $\mathbf{s}(p)$ at which the flow continues to be in the same direction along the trajectory fibre. Since $\mathcal{C}_\tau$ is formed by collecting together all such culmination points, the flow across $\mathcal{C}_\tau$ (at any point) must be in the same sense as that across $\mathcal{C}_+$. The only potential violation to this (keeping in mind that τ is a piecewise differentiable function) occurs if the culminating curve $\mathcal{C}_\tau$ in the diffeomorphic system has a finite number of "cusp points" or "inflection points" as indicated in Fig. 11. The corresponding values of p correspond respectively to $\mathbf{s}'(p)$ being undefined or momentarily parallel to $\mathbf{f}(\mathbf{s}(p))$ — exactly the situations for which "essential uni-directionality" weakens the definition for "uni-directionality" (Definition 9). So one can choose a tubular region around $\mathcal{C}_+$ based on the largest size of the flow box associated with the rectification theorem, and define the corresponding functions T_+ and T_- accordingly.

Condition (b) is easily achievable because of the C^1-smoothness of κ. Since $\mathbf{f} \cdot \nabla\kappa_g > 0$ for any point $\mathbf{r}_+(p) \in \mathcal{C}_+$, the directional derivative

$$\left.\frac{d\kappa_g}{d\ell}\right|_{\ell=0} = \frac{\mathbf{f}(\mathbf{r}_+(p))}{|\mathbf{f}(\mathbf{r}_+(p))|} \cdot \nabla\kappa_g(\mathbf{r}_+(p)) > 0$$

in which ℓ is an arclength parametrisation of the trajectory fibre through $\mathbf{r}_+(p)$ in the direction of the flow, chosen so that $\ell = 0$ at $\mathbf{r}_+(p)$. Since $\kappa_g = 0$ when $\ell = 0$ and but has a strictly positive derivative at this point, there exists $\epsilon_p > 0$ such that for $\ell \in (-\epsilon_p, \epsilon_p)$, $\kappa(\ell)$ is zero only at $\ell = 0$. Using this argument for each p, one can define a fattening of $\mathcal{C}_+$ such that within this fattening, κ is only zero on $\mathcal{C}_+$. Now, choose the intersection of the fattening chosen for condition (a) with the fattening chosen for condition (b) to obtain the needed non-degenerate fattening. □

A.5. Proof of Proposition 1 (flux minimising $\mathcal{C}_+$-generated curve)

Choose a non-degenerate fattening set S_T, and let $\mathcal{C}_\tau$ be a $\mathcal{C}_+$-generated curve lying in S_T, such that $\mathcal{C}_\tau \neq \mathcal{C}_+$. Such a curve is shown in Fig. 9. Note that in this configuration, the set K_g^p must lie to the right of $\mathcal{C}_+$, since by the definition of K_g^+ (the weighted compressibility increasing subset of the weighted incompressible set K_g), the flow must be in the same direction as $\nabla\kappa_g$. Let $\mathbf{x}_i \in \mathcal{C}_+$, $i = 1, 2, 3, \ldots, m$ be the finite number of zeroes of the function τ based on which $\mathcal{C}_\tau$ was generated from $\mathcal{C}_+$ (if there are no zeroes, this step is unnecessary; Fig. 9 shows a situation in which $m = 2$). Define $\mathbf{x}_0 = \mathbf{r}_+(0)$ and $\mathbf{x}_{m+1} = \mathbf{r}_+(1)$, such that the sequence $\{\mathbf{x}_i\}_{i=0}^{m+1}$ is an ordered set of points along $\mathcal{C}_+$. For $i = 0, 1, 2, \ldots, m$, let $\mathcal{C}_+^i \subset \mathcal{C}_+$ be the curve segment with endpoints $\mathbf{x}_i$ and $\mathbf{x}_{i+1}$, and let $\mathcal{C}_\tau^i$ be the part of $\mathcal{C}_\tau$ obtained by applying τ to $\mathcal{C}_+^i$. Since $\mathcal{C}_\tau^i$ lies exclusively on one side of $\mathcal{C}_+$, it will be either in K_g^p or K_g^n. Consider the problem of determining a minimum absolute flux curve among $\mathcal{C}_+^i$-generated curves. Now, if $\mathcal{C}_\tau^i \in K_g^p$, then $\mathcal{C}_\tau^i$ is in a positive fattening set of $\mathcal{C}_+^i$, whereas if $\mathcal{C}_\tau^i \in K_g^n$, then $\mathcal{C}_\tau^i$ is in a negative fattening set of $\mathcal{C}_+^i$. In either case, by Lemma 1, a curve of smaller absolute flux than $\mathcal{C}_\tau^i$ can be found by deforming $\mathcal{C}_\tau^i$ closer and closer towards $\mathcal{C}_+^i$. Thus, among all $\mathcal{C}_+^i$-generated curves in S_T, $\mathcal{C}_+^i$ is the one with the smallest absolute flux. By applying this argument to each of the curve segments, $\mathcal{C}_+$ must be the $\mathcal{C}_+$-generated curve lying in S_T with strictly the smallest absolute flux. □

A.6. Proof of Theorem 2 (flux minimising curve)

It has already been established (Proposition 1) that of all $\mathcal{C}_+$-generated curves lying in a non-degenerate fattening set S_T, $\mathcal{C}_+$ has strictly the smallest absolute flux. This will be extended to all continuous, piecewise differentiable curves connecting $I_{\mathbf{a}}$ and $I_{\mathbf{b}}$, by first extending to an intermediate class of curves.

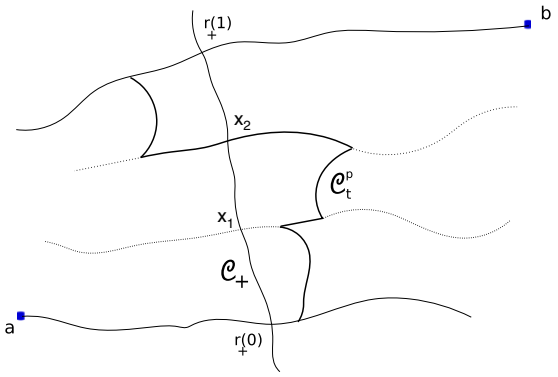

Fig. 10. A piecewise $\mathcal{C}_+$-generated curve (heavy curve), corresponding to τ having two jump discontinuities.

Definition 16 (*Piecewise $\mathcal{C}_+$-Generated Curves*)**.** Let τ be in the class of piecewise differentiable functions on $\mathcal{C}_+$, which are continuous except possibly at a finite number n of points $\mathbf{x}_1, \mathbf{x}_2, \ldots, \mathbf{x}_n$ ordered along $\mathcal{C}_+$ in the direction of increasing p. (The case $n = 0$ corresponds to the situation in which there are no such points of jump discontinuity, in which case τ is continuous.) At each $\mathbf{x}_i$, τ has jump discontinuities, i.e.,

$$\tau_L^i := \lim_{\mathbf{x}\to\mathbf{x}_i^-} \tau(\mathbf{x}) \quad \text{and} \quad \tau_R^i := \lim_{\mathbf{x}\to\mathbf{x}_i^+} \tau(\mathbf{x})$$

are both defined for $i = 1, 2, \ldots, n$ when the limit is taken along $\mathcal{C}_+$. Define

$$\mathcal{D}_\tau := \{\mathbf{y} \in \Omega : \mathbf{y} = \phi(\mathbf{x}, \tau(\mathbf{x})) \text{ for } x \in \mathcal{C}_+ \setminus \{\mathbf{x}_1, \mathbf{x}_2, \ldots, \mathbf{x}_n\}\},$$

which forms a finite number of disconnected curve segments, and

$$\mathcal{E}_\tau^i := \left\{\phi(\mathbf{x}_i, t) : t \in \left[\tau_L^i, \tau_R^i\right] \text{ or } t \in \left[\tau_R^i, \tau_L^i\right]\right\},$$

with the appropriate interval for t being chosen depending on whether $\tau_L^i < \tau_R^i$ or $\tau_L^i > \tau_R^i$ respectively. The class of *piecewise $\mathcal{C}_+$-generated curves* are those curves given by

$$\mathcal{C}_\tau^p := \mathcal{D}_\tau \bigcup \left(\bigcup_{i=1}^n \mathcal{E}_\tau^i\right).$$

Essentially, piecewise $\mathcal{C}_+$-generated curves are generated as follows. The curve $\mathcal{C}_+$ is broken into a finite number of curve segments, and the function τ is continuous on each such segment, which maps to a continuous curve segment within each region in which τ is continuous. These segments are then connected together along the trajectory fibres using the curve segments $\mathcal{E}_\tau^i$, generating a curve $\mathcal{C}_\tau^p$ which is continuous and piecewise smooth. Fig. 10 is an example of such a piecewise $\mathcal{C}_+$-generated curve, associated with a function τ having jump discontinuities at $\mathbf{x}_1$ and $\mathbf{x}_2$. The sets $\mathcal{E}_\tau^1$ and $\mathcal{E}_\tau^2$ in this case are those parts of the heavy curve going along the dotted trajectory fibres passing through these two points. It is obvious that piecewise $\mathcal{C}_+$-generated curves have essentially uni-directional flow, since the flux is uni-directional in all C^1-segments while it is zero along the parts lying along trajectories, with the potential of being undefined at points corresponding to cusps or endpoints in the τ_i.

Lemma 6 (*Flux-Minimising Piecewise $\mathcal{C}_+$-Generated Curve*)**.** *Let S_T be a non-degenerate fattening set of $\mathcal{C}_+$, as guaranteed by Lemma 3. Then, for all piecewise $\mathcal{C}_+$-generated curves $\mathcal{C}_\tau^p \neq \mathcal{C}_+$ in S_T, $\mathcal{C}_+$ has the smallest absolute flux, i.e.,*

$$F_g^a(\mathcal{C}_+) < F_g^a\left(\mathcal{C}_\tau^p\right).$$

Proof. Let $\mathcal{C}_\tau^p$ be a piecewise $\mathcal{C}_+$-generated curve lying in S_T. Suppose the points of discontinuity of the piecewise differentiable function τ on $\mathcal{C}_+$ based on which $\mathcal{C}_\tau^p$ is generated has points of jump discontinuity $\mathbf{x}_i$, $i = 1, 2, \ldots, n$ ordered along $\mathcal{C}_+$. Now, we partition $\mathcal{C}_\tau^p$ into curve segments demarcated by these values (exactly as in the proof of Proposition 1 given in Appendix A.5), and argue (exactly as we did there) that in each segment the corresponding part of $\mathcal{C}_+$ is an absolute flux minimiser. The details will be omitted for brevity. □

Now, suppose $\mathcal{C}$ is an arbitrary piecewise differentiable, continuous curve lying in S_T which connects a point on $I_\mathbf{a}$ to a point on $I_\mathbf{b}$. For each $p \in [0, 1]$, consider the trajectory fibre $\phi(\mathbf{r}_+(p), t)$ passing through $\mathbf{r}_+(p)$. Now, $\mathcal{C}$ must "cross" this at least at one point, since $\mathcal{C}$ must proceed from $I_\mathbf{a}$ to $I_\mathbf{b}$ in a continuous fashion. When using the word "cross" here, it is permitted for $\mathcal{C}$ to continue along the trajectory for a while, before moving on to trajectories corresponding to different p

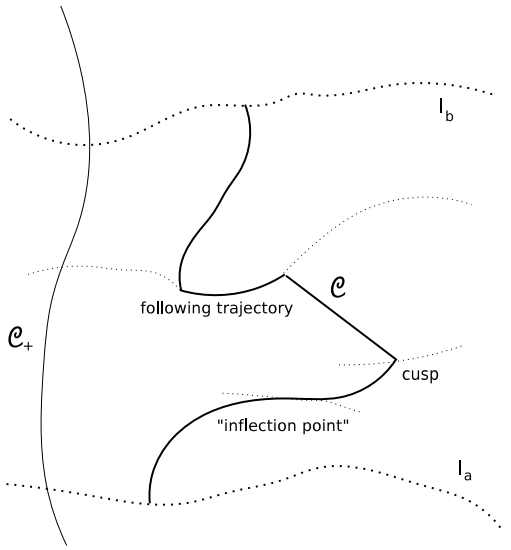

Fig. 11. Points of compromised uni-directionality in a curve $\mathcal{C}$ due to L_g being zero at a point (an "inflection point"), zero in an interval (when following a trajectory) or undefined (a cusp); trajectories are indicated with dotted curves.

values. If $\mathcal{C}$ crosses all such fibres exactly once, then $\mathcal{C}$ is piecewise $\mathcal{C}_+$-generated, and no new work is needed. The difficulty arises if $\mathcal{C}$ crosses a fibre more than once, in other words, if $\mathcal{C}$ reverses its direction in relation to the trajectory fibres at a point, and then has to cross that trajectory fibre later on in the opposite direction. This can be prohibited by insisting on the flow across $\mathcal{C}$ being essentially uni-directional, as in Definition 9, and is similar to the idea of "sneaky returns" defined by MacKay [27].

Lemma 7 (*Essentially Uni-directional and Piecewise $\mathcal{C}_+$-Generated Curves*)**.** *Let $\mathcal{C}$ be a piecewise differentiable continuous curve segment in S_T, parametrised by $\mathbf{s}(q)$ for $q \in [0, 1]$ such that $\mathbf{s}(0) \in I_\mathbf{a}$ and $\mathbf{s}(1) \in I_\mathbf{b}$. Then, the flow across $\mathcal{C}$ is essentially uni-directional if and only if $\mathcal{C}$ is piecewise $\mathcal{C}_+$-generated.*

Proof. The backwards direction of this lemma will be handled first. Points on a $\mathcal{C}_+$-generated curve are either obtained by following the flow from $\mathcal{C}_+$ (in which case the point flux is in the same direction as that of $\mathcal{C}_+$), or by points which follow a trajectory segment (in which case the point flux is zero). It is thus never possible to have two points which have the opposite sign of point flux.

Now suppose the flow across $\mathcal{C}$ is essentially uni-directional. Consider the function $L_g(\mathbf{s}(q))$. This is only undefined when $\mathbf{s}(q)$ fails to be differentiable, so this is a piecewise C^1 function, which takes the same sign (or zero) at all points at which it is defined. Define the sets

$$Q_s := \left\{(q_1, q_2) : L_g(\mathbf{s}(q)) \text{ is sign definite for } q \in (q_1, q_2)\right\},$$
$$Q_0 := \left\{[q_3, q_4] : L_g(\mathbf{s}(q)) = 0 \text{ or is undefined for } q \in [q_3, q_4]\right\},$$

in which $q_1 < q_2$ and $q_3 \leq q_4$. Together, Q_s and Q_0 form alternating intervals which span $[0, 1]$. Each open interval in Q_s can be mapped to $\mathcal{C}_+$ by following the flow. Closed intervals in Q_0 corresponding to an isolated point are those at which either there is an "inflection point" (when the point flux is momentarily zero), or when there is a cusp (at which the flux is undefined). Closed intervals of finite length in which L_g is zero correspond to situations in which $\mathcal{C}$ is following a trajectory. See Fig. 11 for illustrations on these three situation of compromised uni-directionality, corresponding to L_g equalling zero at a point, in an interval, or being undefined at a point. Thus, each interval in Q_0 can be mapped to one point in $\mathcal{C}_+$ by following the corresponding trajectory. This defines a mapping between $\mathcal{C}$ and $\mathcal{C}_+$ which follows the piecewise $\mathcal{C}_+$-generated definition. □

Now consider a general piecewise differentiable, continuous curve $\mathcal{C}$ which connects $I_\mathbf{a}$ to $I_\mathbf{b}$ while remaining in S_T. This is the general situation in Theorem 2. Suppose $\mathcal{C}$ is not piecewise $\mathcal{C}_+$-generated (note that this includes non-simple curves, which will automatically be dealt with by the process to be described). A simple example of such a curve is shown by the heavy curve $\mathcal{C}$ in Fig. 12. Suppose $\mathcal{C}$ is parametrised by $\mathbf{s}(p)$ in which $\mathbf{s}(0) \in I_\mathbf{a}$ and $\mathbf{s}(1) \in I_\mathbf{b}$. Since $\mathcal{C}$ is not $\mathcal{C}_+$-generated, the flow across it is not essentially uni-directional. Consider going along $\mathcal{C}$ until reaching the first point $\mathbf{s}(\bar{p})$ at which the flow reverses; that is, define $\bar{p}$ by

$$\bar{p} = \inf_{p>0} \left\{p : L_g(\mathbf{s}(0))\, L_g(\mathbf{s}(p)) < 0\right\}.$$

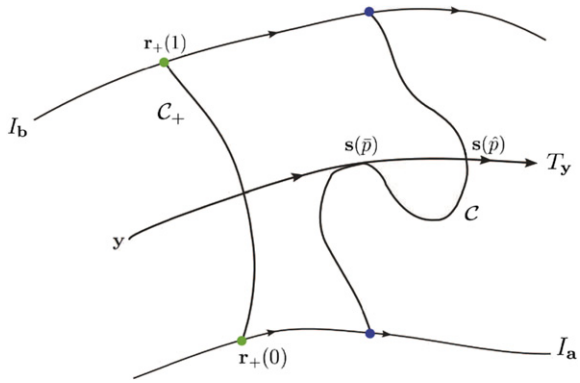

Fig. 12. Reduction of general curves using piecewise $\mathcal{C}_+$-generated curves.

Consider drawing a curve along the trajectory fibre $T_\mathbf{y}$ passing through $\mathbf{s}(\bar{p})$; see Fig. 12, in which this trajectory fibre is that associated with the point $\mathbf{y} \in \mathcal{C}_+$. Now, $T_\mathbf{y}$ must intersect $\mathcal{C}$ at at least one other point, by the fact the curve $\mathcal{C}$ must cross all trajectory fibres emanating from $\mathcal{C}_+$ in proceeding to go from $I_\mathbf{a}$ to $I_\mathbf{b}$. Pick the point $\mathbf{s}(\hat{p})$ at which $\hat{p}$ is chosen to be the *largest* value associated with such a point, i.e.,

$$\hat{p} = \sup_{p \leq 1} \left\{ p : \phi(T_\mathbf{y}, t) = \mathbf{s}(p) \text{ for some } t \in \mathbb{R} \right\}.$$

This ensures that $\mathbf{s}(p)$ never crosses $T_\mathbf{y}$ for $p > \hat{p}$. Note that $\hat{p} > \bar{p}$ (since $\bar{p}$ was chosen as the first point along $\mathcal{C}$ at which $\mathcal{C}$ turns around on itself in relation to the streamlines), and also that $\mathbf{s}(\bar{p})$ and $\mathbf{s}(\hat{p})$ both lie on $T_\mathbf{y}$. Now consider instead of $\mathcal{C}$ the connected curve generated by $\mathbf{s}(p)$ where $0 \leq p \leq \bar{p}$ and $\hat{p} \leq p \leq 1$, with the "link" between $\mathbf{s}(\bar{p})$ and $\mathbf{s}(\hat{p})$ formed along $T_\mathbf{y}$. This curve now has now cut out the multi-valued segment of $\mathcal{C}$ which lies between the two points; see Fig. 12. It is possible to find a continuous function from the part of $\mathcal{C}_+$ which lies between $I_\mathbf{a}$ and $\mathbf{y}$ to the part of $\mathcal{C}$ in which $0 \leq p \leq \bar{p}$, by following trajectory fibres. Now, continue along $\mathcal{C}$ from $\mathbf{s}(\hat{p})$ in the direction of increasing p until reaching another point at which L_g changes sign. Do the same construction at this point, once again cutting out a segment which intersects the trajectory fibres at more than one point. Continue this process until $I_\mathbf{b}$ is reached (only a finite number of such constructions will be necessary, since $\mathcal{C}$ is piecewise C^1). Now, this piecewise $\mathcal{C}_+$-generated curve, along with a union of closed loops, comprises $\mathcal{C}$. Referring to Fig. 12, for example, the new curve along with one anti-clockwise loop gives $\mathcal{C}$. Thus, the absolute flux along the new piecewise $\mathcal{C}_+$-generated curve has strictly a smaller absolute flux that across $\mathcal{C}$. By invoking Lemma 6, this implies that $\mathcal{C}_+$ has a strictly smaller absolute flux than $\mathcal{C}$. □

A.7. Proof of Proposition 2 (flux maximising $\mathcal{C}_-$-generated curve)

This proof is similar to that of Proposition 1, and its details will be skipped. The main difference is that the inequalities become reversed since here $\mathbf{f}$ and $\nabla\kappa_g$ point in opposite directions on $\mathcal{C}_-$. □

References

[1] D.J. Acheson, Elementary Fluid Mechanics, Clarendon Press, Oxford, 1990.
[2] V.I. Arnold, Sur la topologie des écoulements stationnaires des fluides parfaits, C. R. Acad. Sci. Paris 261 (1965) 17–20.
[3] V.I. Arnold, Sur la géométrie differentielle des groupes de lie de dimension infinie et ses applications á lhydrodynamique des fluides parfait, Ann. Inst. Fourier (Grenoble) 16 (1966) 316–361.
[4] V.I. Arnold, Ordinary Differential Equations, The MIT Press, Cambridge, 1973.
[5] S. Balasuriya, Approach for maximizing chaotic mixing in microfluidic devices, Phys. Fluids 17 (2005) 118103.
[6] S. Balasuriya, Optimal perturbation for enhanced chaotic transport, Physica D 202 (3–4) (2005) 155–176.
[7] S. Balasuriya, Optimal frequency for microfluidic mixing across a fluid interface, Phys. Rev. Lett. 105 (2010) 064501.
[8] S. Balasuriya, M.D. Finn, Energy constrained transport maximization across a fluid interface, Phys. Rev. Lett. 108 (2012) 244503.
[9] M. Budišić, I. Mezić, Geometry of the ergodic quotient reveals coherent structures in flows, Physica D 241 (2012) 1255–1269.
[10] L. Cortelezzi, A. Adrover, M. Giona, Feasibility, efficiency and transportability of short-horizon optimal mixing protocols, J. Fluid Mech. 597 (2008) 199–231.
[11] D. D'Alessandro, M. Dahleh, I. Mezić, Control of mixing in fluids: a maximum entropy approach, IEEE Trans. Automat. Control 44 (1999) 1852–1863.
[12] R. Daw, J. Finkelstein, Lab on a chip, Nature 442 (2006) 367.
[13] M. Dellnitz, G. Froyland, C. Horenkamp, K. Padberg-Gehle, A.S. Gupta, Seasonal variability of the subpolar gyres in the southern ocean: a numerical investigation based on transfer operators, Nonlinear Process. Geophys. 16 (6) (2009) 655–663.
[14] M. Dellnitz, O. Junge, On the approximation of complicated dynamical behavior, SIAM J. Numer. Anal. 36 (2) (1999) 491–515.
[15] M. Dellnitz, O. Junge, W.S. Koon, F. Lekien, M.W. Lo, J.E. Marsden, K. Padberg, R. Preis, S.D. Ross, B. Thiere, Transport in dynamical astronomy and multibody problems, Internat. J. Bifur. Chaos Appl. Sci. Engrg. 15 (3) (2005) 699–728.
[16] P. Deuflhard, W. Huisinga, A. Fischer, Ch. Schütte, Identification of almost invariant aggregates in reversible nearly uncoupled markov chains, Linear Algebra Appl. 315 (2000) 35–59.
[17] G. Froyland, Statistically optimal almost-invariant sets, Physica D 200 (2005) 205–219.
[18] G. Froyland, M. Dellnitz, Detecting and locating near-optimal almost-invariant sets and cycles, SIAM J. Sci. Comput. 24 (6) (2003) 1839–1863.

[19] G. Froyland, O. Junge, P. Koltai, Estimating long term behavior of flows without trajectory integration: the infinitesimal generator approach, SIAM J. Numer. Anal. 51 (1) (2013) 223–247.
[20] G. Froyland, K. Padberg, Almost-invariant sets and invariant manifolds — connecting probabilistic and geometric descriptions of coherent structures in flows, Physica D 238 (2009) 1507–1523.
[21] G. Froyland, K. Padberg, M.H. England, A.M. Treguier, Detection of coherent oceanic structures via transfer operators, Phys. Rev. Lett. 98 (22) (2007) 224503.
[22] O. Gubanov, L. Cortelezzi, Towards the design of an optimal mixer, J. Fluid Mech. 651 (2010) 27–53.
[23] G. Haller, I. Mezić, Reduction of three-dimensional volume-preserving flows by symmetry, Nonlinearity 11 (1998) 319–339.
[24] A. Lasota, M.C. Mackey, Chaos, Fractals, and Noise: Stochastic Aspects of Dynamics, second ed., in: Applied Mathematical Sciences, Number 97, Springer, 1994.
[25] Z. Lin, J.-L. Thiffeault, C.R. Doering, Optimal stirring strategies for passive scalar mixing, J. Fluid Mech. 675 (2011) 465–476.
[26] E.N. Lorenz, Deterministic nonperiodic flow, J. Atmospheric Sci. 20 (1963) 130–141.
[27] R.S. MacKay, Transport in 3D volume-preserving flows, J. Nonlinear Sci. 4 (1) (1994) 329–354.
[28] R.S. MacKay, J.D. Meiss, I.C. Percival, Transport in Hamiltonian systems, Physica D 13 (1–2) (1984) 55–81.
[29] G. Mathew, I. Mezić, S. Grivopoulos, U. Vaidya, L. Petzold, Optimal control of mixing in Stokes fluid flows, J. Fluid Mech. 580 (2007) 261–281.
[30] I. Mezić, S. Wiggins, A method for visualization of invariant sets of dynamical systems based on the ergodic partition, Chaos 9 (1) (1999) 213–218.
[31] J.M. Ottino, S. Wiggins, Introduction: mixing in microfluidics, Phil. Trans. R. Soc. A 362 (2004) 923.
[32] A. Pazy, Semigroups of Linear Operators and Applications to Partial Differential Equations, in: Applied Mathematical Sciences, vol. 44, Springer, New York, 1983.
[33] J. Pedlosky, Geophysical Fluid Dynamics, Springer, New York, 1979.
[34] R. Pierrehumbert, Chaotic mixing of tracer and vorticity by modulated travelling waves, Geophys. Astrophys. Fluid. Dyn. 58 (1991) 285–319.
[35] L.V. Polterovich, On transport in dynamical systems, Russian Math. Surveys 43 (1988) 251–252.
[36] C. Schütte, W. Huisinga, P. Deuflhard, Transfer operator approach to conformational dynamics in biomolecular systems, in: Ergodic Theory, Analysis, and Efficient Simulation of Dynamical Systems, 2001, pp. 191–223.
[37] G. Sposito, On steady flows with Lamb surfaces, Internat. J. Engrg. Sci. 35 (1997) 197–209.
[38] M.A. Stremler, S.D. Ross, P. Grover, P. Kumar, Topological chaos and periodic braiding of almost-cyclic sets, Phys. Rev. Lett. 106 (11) (2011) 114101.
[39] J.-L. Thiffeault, G.A. Pavliotis, Optimizing the source distribution in fluid mixing, Physica D 237 (2008) 918–929.
[40] A. Vasilevskiy, K. Siddiqi, Flux maximizing geometric flows, IEEE Trans. Pattern Anal. Mach. Intell. (2002) 1565–1578.
[41] P. Walters, An Introduction to Ergodic Theory, in: Graduate Texts in Mathematics, Number 79, Springer Verlag, New York, 1982.